Hedgehog lipid modifications are required for Hedgehog stabilization in the extracellular matrix

Ainhoa Callejo[§], Carlos Torroja[1§], Luis Quijada and Isabel Guerrero*

Centro de Biología Molecular "Severo Ochoa", C.S.I.C.

Universidad Autónoma de Madrid

Cantoblanco, E-28049 Madrid, Spain.

[§] These two authors contributed equally to this work.

[1] present address:

The Wellcome Trust Sanger Institute

The Wellcome Trust Genome Campus

Hinxton, Cambridge CB10 1SA, UK

***** Corresponding author

Telephone: Office: 34 91 4978492

Lab: 34 91 4978445

Fax: 34 91 49754799

e-mail address: iguerrero@cbm.uam.es

Key words: Hedgehog gradient / *Drosophila* imaginal discs / Hedgehog lipids / HSPG /extracellular-matrix

Running Title: Role of the extracellular matrix in Hedgehog gradient formation

Summary

The Hedgehog (Hh) family of morphogenetic proteins has important instructional roles in metazoan development. Despite Hh being modified by Ct-cholesterol and Nt-palmitate adducts, Hh migrates far from its site of synthesis and programs cellular outcomes depending on its local concentrations. Here, we show that in the receiving cells of the *Drosophila* wing imaginal disc, lipid-unmodified Hh spreads across many more cell diameters than the wild type and this spreading leads to the activation of low but not high threshold responses. Unlipidated Hh forms become internalized through the apical plasma membrane, while wild type Hh enters through the baso-lateral cell surface; in all cases via a dynamin-dependent mechanism. Full activation of the Hh pathway and the spread of Hh throughout the extracellular matrix depend on the ability of lipid-modified Hh to interact with heparan sulfate proteoglycans (HSPG). However, neither Hh-lipid modifications nor HSPG function are required to activate the targets that respond to low levels of Hh.

Introduction

The proteins of the Hedgehog (Hh) family are powerful signaling molecules that act as morphogens, controlling growth and patterning in certain tissues of a range of different organisms at different developmental stages (Ingham and McMahon, 2001). Although the Hh signal molecule was first described as a morphogen in the segmental patterning of the *Drosophila* larva cuticle (Heemskerk and DiNardo, 1994), the Hh morphogen gradient across the wing imaginal disc has provided a unique Hh signaling read out (reviewed in Torroja et al., 2005). In mammals the function of Sonic Hh (Shh) - one of the three members of the Hh protein family (Shh, Indian Hh, and Desert Hh)- as a morphogen has been thoroughly characterized (Echelard et al., 1993; reviewed in McMahon et al., 2003). Shh has been shown

to act as a morphogen in patterning the ventral neural tube (Briscoe et al., 2001; reviewed in McMahon et al., 2003) and in specifying vertebrate digit identities (Ahn and Joyner, 2004; Harfe et al., 2004). Recent works have also revealed an unexpected role of Shh in the control of axon guidance in the developing nervous system (Charron et al., 2003; reviewed in Charron and Tessier-Lavigne, 2005).

Establishing the molecular mechanisms that generate the Hh gradient is essential for our understanding of how the Hh signal elicits multiple responses in a temporally- and spatially specific manner. The Hh spreading mechanism is especially intriguing, because Hh is a lipid-modified molecule. Normally, lipid-modified peptides appear firmly tethered to membranes (Peters et al., 2004). Both in vertebrates and in *Drosophila*, Hh is synthesized as a precursor protein that undergoes a series of postranslational modifications within the secretory pathway that lead to the presentation at the cell surface of the mature and signaling-active Hh (reviewed in Mann and Beachy, 2004). Following cleavage of an amino-terminal signal peptide upon entering the secretory pathway, the Hh protein undergoes an autocatalytic processing reaction that involves internal cleavage between Gly-Cys specific residues (Lee et al., 1994; Tabata and Kornberg, 1994; Bumcrot, 1995). A cholesteryl adduct then covalently binds to the amino-terminal product of this cleavage (Lee et al., 1994; Tabata and Kornberg, 1994; Marti et al., 1995; Porter et al., 1996a; Porter et al., 1996b). The carboxy-terminal domain of the Hh precursor, mediates this auto-processing reaction (Lee et al., 1994; Porter et al., 1995). The second lipid adduct that modifies the Hh protein is palmitic acid, which attaches to the amino-terminal cysteine exposed after signal peptide cleavage (Pepinsky et al., 1998). This acylation is catalyzed by the product of the *sightless* gene, also designated *skinny hedgehog, central missing* or *raspberry* (Amanai and Jiang, 2001; Chamoun et al., 2001; Lee and Treisman, 2001; Micchelli et al., 2002). The doubly lipid-modified Hh is the fully active signaling molecule (Lee et al., 2001). Although much of the Hh maturation process has been determined in

Drosophila, all the metazoan species examined so far show the same biochemical and functional mechanisms.

The importance of lipid modifications has been demonstrated by evaluating the diffusion and signaling properties of different forms of Hh that lack lipid modifications in several animal models. These forms include HhN or ShhN (without the cholesterol moiety) and Hhc85s or Shhc25s (lacking the palmitate modification). While the loss of cholesterol reduces the signaling capabilities in vertebrate models (Porter et al., 1996a; Lewis et al., 2001; Zeng et al., 2001), minor effects have been reported in *Drosophila* wing disc (Burke et al., 1999). However, a detailed analysis in the embryo revealed an essential role for the activation of a specific subset of Hh targets in the embryo (Gallet et al., 2003). The lack of N-terminal acylation dramatically reduces signaling potential, both in *Drosophila* and vertebrates (Chamoun et al., 2001; Kohtz et al., 2001; Lee et al., 2001; Lewis and Eisen, 2001; Gallet et al., 2003; Chen et al., 2004; Tian et al., 2005). The diffusion of *Drosophila* HhN, however, differs from that of their vertebrate counterparts. While cholesterol-free Hh is able to diffuse longer distances in *Drosophila* wing imaginal disc (Burke et al., 1999) but not in *Drosophila* embryos (Gallet et al., 2003), both forms of lipid-unmodified Shh show reduced activity and diffusion properties as measured by analyzing target gene activation and protein distribution (Lewis et al., 2001; Chen et al., 2004; Tian et al., 2005). These differences between *Drosophila* and vertebrates and also in *Drosophila* between the wing imaginal disc and the embryonic epidermis are not well understood, though the effects of lipids on Hh have not yet been systematically explored in *Drosophila* wing imaginal disc cells. Also unclear, are the molecular mechanisms through which a lipid-modified Hh protein is able to diffuse long distances.

Extra-cellular matrix proteins such as heparan sulfate proteoglycans (HSPGs) have been attributed a regulatory role in the signaling activity of secreted morphogen molecules. Thus, the *Drosophila* EXT family of proteins, encoded by the genes *tout velu (ttv), brother of tout velu*

and *sister of tout velu*, essential for the synthesis of HSPGs, are required for the diffusion of lipid-modified Hh (Bellaiche et al., 1998; Bornemann et al., 2004; Takei et al., 2004), yet do not affect the spread of cholesterol-free Hh (Bellaiche et al., 1998; Gallet et al., 2003). EXT proteins are glycosyl transferases that catalyze the formation of heparan sulfate glycosylaminoglycan chains, which are attached to a core protein. Recently, the glypican (a type of HSPG attached to the cell membrane by a GPI-anchor) proteins Dally and Dally-like, were found to be required for Hh diffusion (Han et al., 2004), and Dally-like was also shown to be needed for the reception of Hh in cultured cells and embryos of *Drosophila* (Desbordes and Sanson, 2003; Lum et al., 2003). These data indicate that HSPGs are important for the formation of morphogen gradients and Hh signal reception.

In this work, we analyze the role of Hh lipid modifications (cholesterol and palmitic acid) in spreading, internalization and signaling during Hh gradient formation in the wing imaginal disc. We also examine the function of extracellular matrix HSPGs in the spreading and signaling of lipid-modified and unmodified forms of Hh. Our results indicate that Hh lipid modifications are essential for Hh/HPSG interaction. This interaction is required for the restricted spreading and proper signaling of Hh. We propose a conserved role of lipids in Hh signaling in *Drosophila* and vertebrates.

MATERIALS AND METHODS

Mutants, insertions and transgenes:

A description of the mutations, insertions and transgenes in Fly Base is available at http://gin.ebi.ac.uk:7081.

The mutants used were: *dor*^{8}, a null allele (Shestopal et al., 1997);

shi^{ts1} (Grigliatti et al., 1973) and *hh*^{ts2} (Ma et al., 1993), temperature-sensitive alleles with restrictive temperatures at 32ºC and 29ºC, respectively; and *ttv*$^{l(2)00681}$ (Bellaiche et al., 1998).

The reporter genes used were *dpp-LacZ*$^{BS\ 3.0}$, (Blackman et al., 1991), *dpp*^{10638} (Zecca et al., 1995), and *ptc-lacZ* (a gift from C. Goodman).

The following *Gal4* drivers were used in the ectopic expression experiments using the *Gal4/UAS* system (Brand and Perrimon, 1993): *hh-Gal4* (Tanimoto et al., 2000), *AB1-Gal4* (Munro and Freeman, 2000), *ap-Gal4* (Calleja et al., 1996), and *Ubx-Gal4* (Pallavi and Shashidhara, 2003).

The *hh* transgenes were: *UAS-hh-GFP* (Torroja et al., 2004), *UAS-hhN-GFP* and *UAS-hhc85s-GFP* (Gorfinkiel et al., 2005). After testing the protein expression levels of several lines of GFP-tagged Hh forms by western blot, we selected the lines that showed the same expression levels for each Hh variant (see Fig S1). *UAS-hhN* was prepared for the present study: *UAS-hhN* (Burke et al., 1999), *UAS-hhN* (Tabata and Kornberg, 1994) and UAS- *hhc85s* (Lee et al., 2001) were also used as controls.

Larva genotypes used for generating mosaic clones:

- *Mutant clones:*

Clones were generated by *FLP*-mediated mitotic recombination. Larvae of the corresponding genotypes were incubated at 37ºC for 1 hour 24-48 hours after egg laying (AEL), or for 45 minutes 48-72 hours AEL. The genotypes of the flies for clone induction were:

shi^{ts1} *FRT18A / arm-lacZ FRT18A; FLP/+*

shi^{ts1} *FRT18A / arm-lacZ FRT18A; FLP/+; hh-Gal4 / Hh-GFP(or HhN-GFP or Hhc85s-GFP)*

dor^{8} *FRT18A / arm-lacZ FRT18A; FLP/+; hh-Gal4 / Hh-GFP(or HhN-GFP or Hhc85s-GFP)*

dor^{8} *FRT18A / arm-lacZ FRT18A; ap-Gal4 / Hh-GPF(or HhN-GFP or Hhc85s-GFP); FLP/+*

FLP; FRT 42D ttv^{681b} /FRT 42D arm-lacZ; hhGal4 / Hh-GFP(or HhN-GFP or Hhc85s-GFP)

FLP; FRT 42D ptc^{16}; ttv^{681b} /FRT 42D arm-lacZ; hhGal4 / Hh-GFP

- *Flip-Out clones:*

To generate random clones of *Hh-GFP, Hhc85s-GFP* and *HhN-GFP*, the transgenes *actin>CD2>Gal4* (Pignoni and Zipursky, 1997) and *ubx>f^{+}>Gal4, UAS-ßgal* (de Celis, 1998) were used. Larvae of the corresponding genotypes were incubated at 37^{o}C for 10 minutes to induce *HS-FLP* mediated recombinant clones.

To generate random clones of *Hh-GFP, Hhc85s-GFP* and *HhN-GFP* in an *hh^{ts2}* background, larvae of the genotype: *Act>CD2>GAL4 / HS-FLP122; UAS- Hh-GFP*(or *HhN-GFP* or *Hhc85s-GFP*), *hh^{ts2} / hh^{ts2}* and *y, w, HS-FLP122; ubx>f^{+}>Gal4, UAS-ßgal; UAS- Hh-GFP*(or *HhN-GFP* or *Hhc85s-GFP*), *hh^{ts2} / hh^{ts2}* were incubated at 37^{o}C for 10 minutes to induce recombinant clones and incubated at the restrictive temperature (29ºC) for 18 hours before dissection.

To generate random clone mutants for *ttv* that ectopically expressed Hh and Hh-N under Gal4 control, we used the MARCM technique (Lee and Luo, 1999). Larvae of the following genotypes: *UAS-Hh / y, w, FLP, Tub Gal4 UAS-GFP; FRT 42D ttv^{681b} /FRT 42D tub Gal80* and *y,w, tubGal4 UAS-GFP; FRT 42D Tub Gal80 / FRT 42D ttv^{681b}; UAS-HhN* were incubated at 37ºC for 1 hour 24-48 hours AEL, or for 45 minutes 48-72 hours AEL.

Fractionation of Hh-GFP, HhN-GFP, Hhc85s-GFP, Hhc85sN-GFP in glycerol gradients

Salivary glands were collected in lysis buffer (Tris-HCl 50mM pH 8.0, DOC 0.4%, NaCl 140mM, Triton X-100 1%, EDTA 1mM pH 8.0 containing a cocktail of pepstatin, aprotinin and leupeptin proteases inhibitors) from flies that expressed different forms of Hedgehog-GFP proteins induced with the AB1 Gal4 driver. The lysates (0.1ml) were loaded on a 12 ml linear glycerol gradient (15-50%). The tubes were then centrifuged for 18h at 30000rpm in a SW40 rotor (Beckman) at 4ºC. The gradient was fractionated in 21-23 fractions from the

bottom (50% glycerol) to the top (15% glycerol). An identical gradient was prepared using the standard protein horse ferritin, which has an estimated molecular weight of 465kDa for the multimer. Aliquots were precipitated with TCA, using 10μg insulin as carrier, and analyzed by Western blotting using rat anti-Hh 1/200 (Guillen et al., 1995) and rabbit anti-Hh 1/500 (Tabata and Kornberg, 1994) in the ECL method of immunodetection. The standard protein was developed with its specific antibody.

Immunostaining of imaginal discs and Western blot analysis

Immunostaining was performed according to standard protocols. Antibodies were used at the following dilutions: rabbit polyclonal anti-Hh (Takei et al., 2004) 1:500, mouse monoclonal anti-Ptc (Apa 1.3) (Capdevila et al., 1994) 1/50, rabbit polyclonal anti-ß-gal (from Jackson laboratories) 1/1000, rabbit polyclonal anti-GFP (Molecular Probes, Cat Nº A-6455) 1/100, rabbit polyclonal anti-Col antibody (Vervoort et al., 1999) 1/200, mouse monoclonal anti-En (Patel et al., 1989) 1/100, rat monoclonal anti-Ci (Motzny and Holmgren, 1995) 1/5, rat polyclonal anti-Caupolican (Diez del Corral et al., 1999) 1/100 and mouse monoclonal anti-DE-Cad (Iowa University Hybridoma Bank) 1:50.

For the Western blots, protein extracts from salivary glands of *AB1-Gal4/UAS-Hh*, *UAS-Hh-GFP* flies were prepared in Laemmli buffer, resolved by SDS-PAGE, immuno-blotted and then analyzed using anti-Hh (1/500, Tabata and Kornberg, 1994), rat polyclonal anti-Hh (1/200, Guillen et al., 1995) and anti-GFP (1/1000, Molecular Probes, Cat Nº A-6455) antibodies. The signal was developed using the ECL Western Blotting Analysis System (Amersham Pharmacia). The presence of horse Ferritin was established using a specific antibody (1:1000, Jackson ImmunoResearch Laboratories). The amount of protein extract loaded for each sample was control by Coomasie staining of the SDS-PAGE gel.

The protocols used for labeling the endocytic compartment and extra-cellular labeling of Hh-GFP are described in Strigini and Cohen, 2000, Entchev et al., 2000 and Torroja et al., 2004.

Microscopy and image processing

Brightfield microscopy imaging was performed using an Axioskop 2 plus (Zeiss) microscope, coupled to a CCD camera. A laser scanning confocal microscope (LSM 510 META; MicroRadiance and Radiance 2000) was used for confocal fluorescence imaging.

Metamorph and Image J software were used for image processing and determining fluorescence levels.

Results

Lipid-modifications are required for correct Hh gradient formation

In larvae, the wing imaginal disc is formed by epithelial cells with a sac-like structure. One surface of this structure comprises a monolayer of columnar epithelial cells with their apical membranes orientated towards the disc lumen. This specialized group of cells will give rise to the wing (and notum). The other overlying surface is a squamous epithelium, called the peripodial membrane, which does not develop into any cuticular structure in the adult fly (see diagrams in Fig. 5). Two populations of cells with different adhesion affinities divide the epithelium of columnar cells into posterior (P) and anterior (A) cells (García-Bellido et al., 1973). Hh is synthesized in P cells and the processed HhNp 20 kD lipid-modified molecule is able to diffuse several cell diameters away, despite its potential to tether to membranes. However, the spreading of Hh is limited by interaction with the Patched (Ptc) receptor that is expressed in the A cells. When Hh reaches Ptc, a concentration gradient of Hh is formed at the boundary that separates the anterior and posterior (A/P) compartments (reviewed in Ingham and McMahon, 2001; Torroja et al., 2005). Here, we explored the role of lipid moieties in the spreading and signaling mechanisms of the Hh molecule in the wing imaginal disc. To this end,

we engineered GFP-tagged versions of the different Hh variants: HhN (lacking cholesterol), Hhc85s (lacking palmitic acid), and Hhc85sN (lacking cholesterol and palmitic acid) and then compared their functions with that of fully lipid-modified Hh-GFP. The correct processing of Hh-GFP and of variants lacking lipid-modifications was checked in Western blots, which showed bands of expected molecular weight for each protein (Fig. S1A).

Biochemical studies in tissue cultured cells have shown that Shh, the vertebrate ortholog of *Drosophila* Hh, can form multimeric complexes in which hydrophobic moieties are thought to be sequestered inside the multimer to make the complex soluble and diffusible (Zeng et al., 2001; Chen et al., 2004). This multimeric complex shows stronger signaling activity than Shh monomers and both lipid modifications are essential for its formation (Chen et al., 2004). Hh multimers have been isolated from S2 cells, a *Drosophila* cell line, but surprisingly, palmitic acid modification was not essential for Hh to form a multimeric complex in S2 cells (Chen et al., 2004). Thus, we decided to establish whether the lipid-modified and unmodified forms of Hh-GFP expressed in fly tissues could form a multimeric complex. To avoid possible interaction with endogenous Hh, we ectopically expressed the different Hh-GFP forms in salivary gland cells, where there is no endogenous Hh (Zhu et al., 2003). Fig. 1A shows that only the lipid-modified Hh-GFP was able to form multimers. As a control, we repeated the experiment using GFP-untagged versions of Hh and obtained similar results (data not shown). These data are in agreement with vertebrate Shh multimerization but not with previous results suggesting that the palmitic modification is not required for the formation of a multimeric complex in *Drosophila* tissue culture cells (Chen et al., 2004). This discrepancy might be due to the experimental approach employed (see Materials and Methods).

In Hh-GFP/HhGal4 wing discs, dots of Hh-GFP, which we previously identified as endocytic vesicles of Hh internalized by Ptc (Torroja et al., 2004), were observed at a distance of five, six or even more cell diameters in the A compartment close to the A/P border. Discs

expressing HhN-GFP, Hhc85s-GFP (Figs. 1C and D) and even Hhc85sN-GFP (data not shown) also showed these dots distributed throughout the whole A compartment. These GFP accumulations observed for HhN-GFP and Hhc85s-GFP were also detected using several anti-Hh antibodies (Figs. S1 B and b, C and c).

We then tried to establish if these punctate structures were vesicles of the endocytic compartment or extracellular aggregates -it has been suggested that Hh multimers could form extracellular aggregates, called Large Punctuated Structures (LPS), in the embryo (Gallet, 2003; Gallet, 2005)-. Discs expressing different Hh-GFP variants induced with Hh-Gal4 were incubated "in vivo" with dextran-red to label the endocytic compartment. We found extensive co-localization of Hh-GFP, Hhc85s-GFP and HhN-GFP (as well as Hhc85sN-GFP) with the internalized dextran-red (Figs. 1B-D and b-d, arrowheads and data not shown). To check whether the dots of Hh-GFP that did not co-localize with dextrans (Figs. 1b-d, arrows) were intracellular or extracellular, we simultaneously labeled the extracellular Hh-GFP with α-GFP antibody and the endocytic vesicles with dextrans. Fig. S1D shows that the punctate structures of Hh-GFP that did not co-localize with dextrans (arrows) are indeed intracellular vesicles. This indicates that all Hh variants dots correspond to accumulations in the endocityc compartment.

Lipid-modifications localize Hh at the lateral plasma membrane of receiving cells

We and others previously reported that Ptc internalizes Hh through a dynamin-dependent mechanism, because there was build-up and co-localization of Hh and Ptc when endocytosis was blocked in the temperature-sensitive *dynamin* mutants, *shibire*^{ts1} (*shi*^{ts1}), both in the fly embryo and in imaginal disc cells (Capdevila et al., 1994; Han et al., 2004; Torroja et al., 2004; Gallet and Therond, 2005). We observed that the endocytosed Hh was targeted by the lysosomal protein degradation pathway because Hh and Ptc also accumulated in clones of *dor*$^{-}$ mutant cells induced in imaginal discs (Torroja et al., 2004), a mutation that blocks the

ubiquitin pathway (Sevrioukov et al., 1999). Since the lipid-unmodified forms of Hh do not form a gradient in the wing disc (Figs. 1C and D), we then tried to determine whether the mechanisms of internalization and degradation of HhN-GFP and Hhc85s- GFP were affected.

We induced *shi*^{ts1} mutant clones in discs expressing the variant forms of Hh in the P compartment and observed that Hhc85s-GFP and HhN-GFP accumulated at the apical membrane of *shi*^{ts1} mutant clones at the restrictive temperature (Figs. 2B, C and E), while Hh-GFP built up at the baso-lateral membrane (Figs. 2A and D). This distinct apico-basal accumulation in Hh and HhN or Hhc85s in *shi*^{ts1} clones suggests that the mutant forms diffuse through the apical surface of the epithelium, while wild type Hh diffuses through the basolateral surface. To visualize the diffusion of Hh, we compared the extracellular staining of Hh-GFP with that of the mutant forms in wing imaginal discs expressing the GFP fusion proteins in the P compartment. Figure 3 shows the presence of the three proteins on the apical surface in the producing cells (Figs. 3 A, B, C asterisk). Surprisingly, only the mutant forms were able to diffuse through the apical surface towards the A compartment, while no apical labeling was found for Hh-GFP in the A compartment (Figs. 3 A, B and C apical arrows). On the other hand, Hh-GFP diffused and formed an extracellular gradient in the baso-lateral space (Fig. 3 A baso-lateral arrowhead), while the mutant forms of Hh were much less represented and no extracellular gradient or build up were observed (Figs. 3 B and C baso-lateral arrowheads).

Intracellular accumulation of Hh was also visualized when degradation was blocked in *dor*^{8} clones. In the A compartment clones, massive accretion of Hh-GFP, HhN-GFP and Hhc85s-GFP was observed (Figs. 4A-C). Surprisingly, important differences were found between wild type and mutant Hh forms. The amount of wild type Hh deposition was found to be directly related to the amount of Ptc (see graph in Fig. 4A). However, there was no such relationship for HhN or for Hhc85s, given that there was an accumulation of Hh but not of Ptc

in these clones (see Figs. 4B and C and graphs). This uncoupling between Ptc and Hh build up suggests distinctive Hh internalization and degradation mechanisms independent of Ptc. To explore this hypothesis, we induced *dor*^{8} clones in a wing disc expressing the various forms of Hh-GFP fusion proteins in the dorsal compartment. In this model, we can examine the internalization and degradation of Hh-GFP forms in the P compartment where there is no Ptc. As predicted, both HhN-GFP and Hhc85s-GFP were targets for degradation both in the A compartment and P compartment (Figs. 4 E and F), while wild type Hh-GFP is only degraded when Ptc is present (Fig. 4 D and Torroja et al., 2004). A small amount of Ptc accumulation was still observed in *dor*^{8} clones expressing HhN-GFP but not Hhc85s-GFP (Figs. 4 E and F). This last result indicates less interaction of Hhc85s with Ptc and could explain the much lower response exerted by this form of Hh in terms of target activation compared to HhN.

Several conclusions can be derived from the above results. First, the non-palmitoylated and the non-cholesterolated forms of Hh synthesized in the P compartment (or in the dorsal compartment) are freely distributed and internalized throughout the disc. Second, internalization of wild type Hh occurs through the basolateral membrane while internalization of the lipid-unmodified forms takes place through the apical plasma membrane; in all cases via a dynamin-dependent mechanism. Third, Ptc independent internalization of the lipid-unmodified forms of Hh also induces the Ptc independent degradation of Hh. This Ptc-independent mechanism of Hh internalization was previously suggested both in imaginal disc cells (Torroja et al., 2004) and in the embryo (Gallet and Therond, 2005).

Since the internalization of HhN-GFP and Hhc85s-GFP occurred throughout the disc epithelium via the apical plasma membrane, even for areas of the disc far away from the Hh producing cells, our interpretation was that these secreted forms of Hh could not be properly retained by the extracellular matrix. Hence, it was very likely that Hh forms not modified by lipids would concentrate in the disc lumen after their secretion, escaping the spatial restriction

imposed by the extracellular matrix. To test this hypothesis, we expressed Hh-GFP, HhN-GFP and Hhc85s-GFP only in peripodial membrane cells using the *ubx-Gal4* line (Pallavi and Shashidhara, 2003) and determined whether these forms of Hh can travel through the lumen and be internalized by the disc proper cells. When we expressed HhN-GFP and Hhc85s-GFP with the *ubx-Gal4* driver we observed Hh vesicles in the disc proper cells (Figs. 5B-c') while no vesicles were observed in the case of wild type Hh (Figs. 5A, a and A', a'). HhN endocytosis was more evident in the A than in the P compartment (Figs. 5B' and b'), indicating that although there is Ptc independent internalization of HhN, Ptc is still able to interact with HhN, as is also reflected by its signaling properties. Thus, HhN-GFP expressed from the peripodial membrane was able to induce the activation of gene targets, such us *dpp-LacZ* in the disc proper cells (Fig. 5B'). However, Hh-GFP was unable to induce this distant activation of response genes (Fig. 5A'). This non-autonomous effect of HhN-GFP from peripodial to disc proper cells through the disc lumen was also patently manifested by the enlargement of the A compartment (Fig. 5 B') and by the adult phenotypes (Fig. 5E and G). Flies expressing HhN-GFP in the peripodial membrane (but not those expressing Hh-GFP) showed extra veins and enlargement of the costa region of the wing (Fig. 5E), and extra bristles in the notum (Fig. 5G). These mutant phenotypes are similar to those observed as a consequence of ectopic activation of the Hh pathway (Basler and Struhl, 1994; Tabata and Kornberg, 1994) and in hypomorph Ptc alleles (Rogert et al., 1992; Capdevila et al., 1994).

The fact that lipid unmodified Hh can diffuse from the peripodial membrane rise the question of whether the extended diffusion of these forms, seen when expressed in its own domain with the *hh-Gal4* driver, is produced as a consequence of its release solely by the peripodial cells. However, these forms still generate more extended gradient than wild type Hh when expressed with the Ap-Gal4 driver (that is expressed solely in the disc proper cells, Fig. 4) or when single clones are generated in the wing disc proper cells (see Fig. S2).

These results indicate that lipid-unmodified Hh is poorly retained by the extracellular matrix both in the peripodial cells and in the disc proper cells and is released to the lumen where it can freely diffuse.

Lipid modifications to Hh are required to activate high threshold responses

We previously described that Hh-GFP is able to signal as wild-type Hh (Torroja et al., 2004). We next analyzed the behavior of lipid-free Hh-GFP molecules in clones of cells ectopically expressing each form of Hh in the wing imaginal disc. For all the experiments we chose fly lines that expressed similar levels of the various forms of Hh-GFP. As a control, we also induced ectopic expression clones of GFP-untagged versions and observed the same responses as with the GFP-tagged forms (data not shown). Ectopic Hh-GFP expressing clones in the A compartment of the wing imaginal disc induced all Hh responses, both autonomously (arrows) and non-autonomously (arrowheads), indicating that Hh-GFP is able to signal at the same distance from its source as the wild-type Hh protein (Figs. 6C-F and Torroja et al., 2004). Although Hh is not expressed in A compartment cells, we previously reported that ectopic Hh in the A compartment is able to activate endogenous Hh expression (Guillen et al., 1995). Hence, to avoid possible interaction of ectopic Hh with endogenous Hh, we also induced clones of all Hh forms in a hh^{ts2} background at the restrictive temperature and obtained the same results. Ectopic Hhc85s-GFP clones in the A compartment did not activate *en* (Fig. 6K) but activated other Hh targets such as *ptc* (at very low levels and only cell autonomously) and *dpp* (also at low levels), both autonomously and non-autonomously (Figs. 6 L-N). HhN-GFP, however, was able to activate all the Hh targets, although in the case of *en* and *ptc* the non-autonomous activation was very short-range (only one cell diameter outside the clone) (see arrowheads in Figs. 6G and H, arrowheads). Surprisingly, low threshold responses such as *dpp*, *Iro* and the cytoplasmatic stabilization of *Ci*, were activated throughout the disc, even though

HhN-GFP induction occurred in a restricted clone (Figs. 6 I, J and data not shown). This differential non-autonomous response between low- and high-threshold response target genes with cholesterol-unmodified Hh was unexpected (see diagrams in Figs. 6 O, P and Q).

Low interaction of the lipid-unmodified forms of Hh with HSPGs

There is compelling evidence that Hh moves through the extracellular matrix and it has been argued that HSPGs are required for the stable retention of Hh on the cell surface. This results in restricted movement through the surface of the epithelium (Bellaiche et al., 1998; The et al., 1999; Bornemann et al., 2004; Han et al., 2004; Tabata and Takei, 2004; Takei et al., 2004; Glise et al., 2005; Gorfinkiel et al., 2005). Since we observed greater Hh-N spreading and lower signaling than the wild type Hh, we then analyzed the role of HSPGs in the movement and signaling of HhN-GFP compared to Hh-GFP. As previously published (Bellaiche et al., 1998), lipid-modified Hh was only able to activate its targets in the first row of cells touching the P compartment, reflecting problems in Hh stabilization and diffusion in *ttv*$^{-}$ clones (Fig. 7A-D). Accordingly, we observed Hh-GFP endocytic vesicles only in this first row of cells of a *ttv*$^{-}$ mutant clone (Fig. 7A arrowheads). These vesicles co-localized with Ptc, indicating that Ptc mediates the internalization of Hh-GFP. This finding was reinforced by the fact that Hh-GFP vesicles disappeared in *ttv, ptc* double mutant clones (Fig. S3B). HhN-GFP and Hhc85s-GFP, however, were able to move through a *ttv*$^{-}$ clone, as shown by the GFP punctate structures (Fig. 7 E, I arrows). In terms of signaling, HhN-GFP was able to rescue, in all cells inside the clone, Hh low-threshold responses, such as high levels of Ci (data not shown) or the activation of *iro* (Fig. 7G, arrowhead, see also clone 1 in H), but not high-threshold targets of Hh signaling, such as Ptc or Col (Fig. 7E and F). We observed, however, that *ttv*$^{-}$ clones located distant to the A/P border were not able to activate *iro* (Fig. 7G arrow, and clone 2 in H), indicating that some interaction still exists between HSPGs and HhN. In conclusion, these results suggest that the

diffusion of lipid-unmodified forms of Hh and the activation of their targets are less restricted by HSPG function than in the case of fully lipid-modified Hh.

HSPGs are specifically required for the high-threshold Hh response

Since HhN-GFP was able to move across a *ttv*$^{-}$ mutant clone and activate low-threshold Hh targets, we wondered whether HSPG function was required for maximal activation of the Hh pathway. HSPGs have been previously also implicated in the reception of Hh by responsive cells. Thus, the glypican Dally-like is known to be required for Hh reception in embryos and tissue culture cells (Desbordes and Sanson, 2003; Lum et al., 2003; Lin, 2004). We used the MARCM technique (Lee and Luo, 1999) to generate clones of *ttv*$^{-}$ cells that simultaneously express high levels of the fully lipid-modified Hh. Target genes that respond to high levels of Hh were not expressed inside these clones, although activation in the first row of cells within the clone was observed (Figs. 8 A, A' and B, B', arrowheads). This activation of high-threshold response genes in the first row of cells inside the clone was also shown in *ttv*$^{-}$ clones (that did not simultaneously express Hh) abutting the A/P border (Figs. 7A, B). This suggests a possible non-autonomous interaction between the Ptc receptor expressed in the cells of the clone and the HSPGs of wild-type cells surrounding the clone. Interestingly, target genes responsive to low levels of Hh were still activated despite the absence of *ttv* function (Figs. 8 C, C' and D, D'). When we analyzed *ttv*$^{-}$ clones that expressed HhN, the same autonomous responses were observed as when we used fully lipid-modified Hh (data not shown). All these results indicate that HSPG function is required for maximal activation of the Hh pathway at the reception level.

Discussion

This work indicates that interaction between lipid-modified Hh and HSPGs is required to restrict the movement of Hh throughout the extracellular matrix and promote optimal

activation of the Hh pathway. This finding is based, first, on the analysis of the spreading and signaling properties of the lipid-unmodified forms of Hh, and secondly on the responses shown by cells mutant for the genes that synthesize HSPGs to lipid-modified and unmodified forms of Hh.

One of the first observations made when expressing the lipid-unmodified forms of Hh is an extended gradient compared to that elicited by wild type Hh (Figs. 1 B-D). It is known that Hh gradient formation depends on the presence of its receptor Ptc, which is responsible for the internalization and degradation of Hh (reviewed in Torroja et al., 2005). Thus, we analyzed the internalization and degradation of lipid-unmodified forms of Hh, in the search for an explanation for the vast expansion of the gradient. We found that these mutant forms of Hh were efficiently internalized and degraded throughout the disc. So, why is there an extended gradient? One clue emerged from our analysis of Hh internalization in *shi* mutant cells. We found that the lipid-unmodified forms of Hh were internalized through the apical side of the epithelium, while wild type Hh is internalized mainly through the basolateral surface. This differential internalization matches the preferential localization of lipid-unmodified Hh at the apical surface plasma membrane of A compartment cells. We also found that the lipid-unmodified forms of Hh can be internalized and degraded through a Ptc-independent mechanism. Thus, it might well be that this Ptc-independent mechanism would have no positive feedback from Hh, and would therefore not work as efficiently as when internalization was mediated by Ptc (see Lander et al., 2002), or just a lower rate of internalization and degradation than Ptc. Alternatively or in addition, a reduced restriction of spreading through the extracellular matrix could explain why the gradient is extended. In agreement with this, we observed that the localization of lipid-unmodified Hh is not affected in mutants for HSPGs (data not shown). Further, Hh is less represented at the baso-lateral membrane in the absence of HSPGs (Fig 6 in Gorfinkiel et al., 2005) indicating an active role

of HSPGs in anchoring lipid-modified Hh in the lateral cell region. This conclusion is further supported by the localization of the glypican Dally-like at the baso-lateral membrane of wing imaginal disc cells (Baeg and Perrimon, 2000; Han et al., 2005).

If the interaction of dual lipid modified Hh with HSPGs is important for Hh retention, then we would expect to see the same phenotype if we removed the lipids from Hh as *ttv* mutants, that is, the extended movement of Hh. This possibility could only be demonstrated using a whole disc mutant for *ttv*, which is difficult to obtain because *ttv* mutants are larval lethal. A further possibility would be to use a hypomorphic mutation of *ttv*, which is not available for *Drosophila*. In mice, in which an Ext1 hypomorphic mutant already exists, it has been demonstrated that this is indeed the case and Ihh signaling during embryonic chondrocyte differentiation shows an extended range (Koziel et al., 2004).

In the formation of the Hh morphogenetic gradient throughout the extracellular matrix, we have to consider not only the function of HSPGs rendering a restricted space suitable for the spreading of Hh (reviewed in Lin, 2004; Tabata and Takei, 2004) but also a possible role of HSPGs in signal reception. Thus, if a specific HSPG acts as a co-receptor for Hh together with Ptc, binding the ligand to the HSPG and to the receptor, it could limit the range of ligand movement and at the same time boost the signaling process. In effect, compelling evidence in the fly embryo and in fly tissue culture cells it indicates that the presentation of Hh to Ptc might require a specific HSPG such as Dally-like (Desbordes and Sanson, 2003; Lum et al., 2003). In this sense, we show here that HSPG function is required for Hh reception also in the imaginal disc, but only to trigger Hh high-threshold response genes (Figs. 7 and 8). Thus, it is plausible that Hh coupled to a specific HSPG could form a high-affinity complex together with Ptc to allow these high-threshold responses. On the other hand, we observed that in the wing imaginal disc, Hh lacking cholesterol was able to induce the same low responses as fully lipid-modified Hh, in both cases in an HSPG-independent manner. This suggests that the low-level response of

the pathway might involve a different reception complex in which HSPGs are not necessary.

Two different mechanisms of Hh target gene activation have been also proposed in the ectoderm of *Drosophila* embryos. These mechanisms correlate with asymmetric cellular responses to Hh signaling. Hh requires the cholesterol modification for a maximal response of the pathway, i.e., for the activation of Wingless (Wg) and Ptc in anteriorly located cells (compartment border), but cholesterol is dispensable for the activation of Rhomboid (Rho) and Ptc in posteriorly located cells (segmental border) (Gallet et al., 2003). Moreover, *ttv* function is needed only for activating target genes in anterior cells (Wg) (The et al., 1999) and not for target genes posterior to the Hh source (Rho) (Gallet et al., 2003). This result was interpreted as a requirement for Hh movement towards anteriorly located cells to activate Wg. Based on the requirement of *ttv* for Hh high threshold responses in wing imaginal disc cells, we anticipate that *ttv* is required in the embryonic epidermis for the reception of Hh in the activation of certain Hh target genes but not others. This differential activation of Hh targets in the embryonic ventral epidermis and wing imaginal disc cells is known to be dependent on *fused* (*fu*) activity (Sanchez-Herrero et al., 1996; Ohlmeyer and Kalderon, 1998; Therond et al., 1999; Mullor and Guerrero, 2000). Hence, it is possible that this differential activation of the Hh pathway could be exerted through different structures of the Hh receptor complex. Thus, Ptc plus a glypican, possible Dlp, could act as a high-affinity receptor whose activation would then be mediated by Fu kinase, while Ptc without Dlp could act as a low-affinity receptor whose activation was independent of Fu.

Also in the embryonic epidermis, it has been proposed that apically distributed Hh LPSs are needed to activate Wg in anterior cells (Gallet et al., 2003). However in the wing disc, we observed that all forms of Hh produced punctate structures, both apical and baso-lateral, which are also observed using different Hh antibodies. These structures are endocytic vesicles and are the result of the accumulation of Hh in the endocytic compartment rather than the visualization

of multimeric lipid-modified Hh complexes moving from one cell to another. The high accretion of Hh observed in the *dor*$^{-}$ clones indicates that these large endocytic vesicles are targeted to the degradation pathway.

Hh lipidation seems to confer a specific conformation to the Hh molecule so that it is targeted to specific locations in the receiving cells for signaling. Hence, the Ptc receptor might be located in sterol-rich membrane microdomains or lipid rafts in *Drosophila*, which function as platforms for intracellular sorting and signal transduction (Rietveld et al., 1999, reviewed in Incardona and Eaton, 2000). Hh without lipids might not recognize these platforms resulting in less efficient signaling. Interestingly, we observed the internalization of the lipid-unmodified Hh that was not mediated by Ptc, more striking in the case of Hhc85s. HhN has less potency to activate the Hh pathway than wild type Hh; as previously reported (Lee et al., 2001; Gallet et al., 2003); we have found that Hhc85s is much less potent than HhN (Fig.6) and Hhc85sN is even less potent (data not shown). As we have shown, this low response in terms of target activation of unlipidated forms of Hh could be explained by their diminished access to Ptc.

The literature contains several contradictory conclusions regarding the signaling functions of Hh lipids in the mouse and *Drosophila*. Thus, the elimination of cholesterol has been reported to have a major effect on Hh signaling in vertebrates but only minor effects in *Drosophila* (Porter et al., 1996a; Burke et al., 1999). On the other hand, the diffusion of *Drosophila* HhN and Hhc85s differs from that of their vertebrate counterparts. In vertebrates, forms of Shh lacking cholesterol or palmitic acid showed restricted signaling and diffusion (Lewis et al., 2001; Chen et al., 2004), while in *Drosophila*, Hh without lipids is able to diffuse longer distances (Porter et al., 1996a; Burke et al., 1999). It is likely that the different structural characteristics of the target tissues where Hh acts could account for differences in the lipid requirements of signaling and diffusion between *Drosophila* and vertebrates. The wing imaginal disc consists of a single-layered sac of polarized epithelial cells with their apical

surfaces orientated towards the disc lumen. If the extracellular matrix were not able to retain lipid-unmodified Hh, this molecule would be delivered to the disc lumen. The peculiar structure of the wing disc concentrates the lipid-unmodified forms of Hh in the lumen and is likely to promote the activation of low-threshold target genes cells far away from the Hh producing cells. A role for the luminal transmission of ligands was already described for Dpp signaling in *Drosophila* wing disc (Gibson et al., 2002). Here, we show that only lipid-unmodified Hh can travel from the peripodial membrane to the disc proper cells (Fig. 5). Our results indicate that wild type Hh is not traveling from the peripodial membrane towards the wing disc. In other systems, Hh without lipids might be lost because it is not retained by the extracellular matrix; therefore, it would be expected that very restricted diffusion and signaling of non lipid-modified forms of Hh occurs, as demonstrated by Chamoun et al., 2001; Kohtz et al., 2001; Lee et al., 2001; Lewis and Eisen, 2001; Chen et al., 2004. Our results indicate that the role of lipids in Hh signaling is similar in *Drosophila* and vertebrates and corroborate the previous notion that lipid-modified forms of Hh are predominantly membrane-associated, and that Hh mutated forms lacking lipid adducts dissociate from cells after secretion (Lee et al., 1994; Porter et al., 1995; Pepinsky et al., 1998; Peters et al., 2004). In summary, we conclude that dual lipid modification, by cholesterol and palmitic acid, appears to be critical for interaction between Hh and HSPGs as well as Ptc receptor, and that these interactions are important both for the stable retention of Hh and for proper signaling.

Acknowledgments

We are very grateful to Nicole Gorfinkiel, Kiki Lalioti and Ignacio Sandoval for their help and discussions, to Carmen Ibañez for her excellent technical assistance and to Ernesto Sánchez-Herrero and Aphrodite Bilioni for comments on the manuscript. We also thank T. Tabata for the anti-Hh antibody, A. Vincent for the anti-Col antibody, R. Holmgren for the anti-Ci antibody and J. Modolell for the anti-caupolican antibody. Fly strains were provided by X. Lin,

L S Shashidhara, J. Treisman, S. Zipursky, G. Morata, K. Basler, T. Kornberg, H. Kramers, JF de Celis, T. Tabata and the Bloomington stock center. This study was financed by the Spanish D.G.I.C.Y.T, grants BFU2005-04183/BMC and MCYT GEN2001-4846-C05-01, the Comunidad Autónoma de Madrid, grant GR/SAL/0185/2004, and by an institutional grant from the Fundación Areces.

References:

Ahn, S. and Joyner, A. L. (2004). Dynamic changes in the response of cells to positive hedgehog signaling during mouse limb patterning. *Cell* **118**, 505-16.

Amanai, K. and Jiang, J. (2001). Distinct roles of Central missing and Dispatched in sending the Hedgehog signal. *Development* **128**, 5119-27.

Baeg, G. H. and Perrimon, N. (2000). Functional binding of secreted molecules to heparan sulfate proteoglycans in Drosophila. *Curr Opin Cell Biol* **12**, 575-80.

Basler, K. and Struhl, G. (1994). Compartment boundaries and the control of Drosophila limb pattern by hedgehog protein. *Nature* **368**, 208-14.

Bellaiche, Y., The, I. and Perrimon, N. (1998). Tout-velu is a Drosophila homologue of the putative tumour suppressor EXT-1 and is needed for Hh diffusion. *Nature* **394**, 85-8.

Blackman, R. K., Sanicola, M., Raftery, L. A., Gillevet, T. and Gelbart, W. M. (1991). An extensive 3' cis-regulatory region directs the imaginal disk expression of decapentaplegic, a member of the TGF-beta family in Drosophila. *Development* **111**, 657-66.

Bornemann, D. J., Duncan, J. E., Staatz, W., Selleck, S. and Warrior, R. (2004). Abrogation of heparan sulfate synthesis in Drosophila disrupts the Wingless, Hedgehog and Decapentaplegic signaling pathways. *Development* **131**, 1927-38.

Brand, A. H. and Perrimon, N. (1993). Targeted gene expression as a means of altering cell fates and generating dominant phenotypes. *Development* **118**, 401-415.

Briscoe, J., Chen, Y., Jessell, T. M. and Struhl, G. (2001). A hedgehog-insensitive form of patched provides evidence for direct long-range morphogen activity of sonic hedgehog in the neural tube. *Mol Cell* **7**, 1279-91.

Bumcrot, D. A., Takada, R. and McMahon, A. P. (1995). Proteolytic processing yields two secreted forms of Sonic hedgehog. *Molecular and Cellular Biology* **15**, 2294-2303.

Burke, R., Nellen, D., Bellotto, M., Hafen, E., Senti, K. A., Dickson, B. J. and Basler, K. (1999). Dispatched, a novel sterol-sensing domain protein dedicated to the release of cholesterol-modified hedgehog from signaling cells. *Cell* **99**, 803-15.

Calleja, M., Moreno, E., Pelaz, S. and Morata, G. (1996). Visualization of gene expression in living adult Drosophila. *Science* **274**, 252-5.

Capdevila, J., Pariente, F., Sampedro, J., Alonso, J. L. and Guerrero, I. (1994). Subcellular localization of the segment polarity protein patched suggests an interaction with the wingless reception complex in Drosophila embryos. *Development* **120**, 987-98.

Chamoun, Z., Mann, R. K., Nellen, D., von Kessler, D. P., Bellotto, M., Beachy, P. A. and Basler, K. (2001). Skinny hedgehog, an acyltransferase required for palmitoylation and activity of the hedgehog signal. *Science* **293**, 2080-4.

Charron, F., Stein, E., Jeong, J., McMahon, A. P. and Tessier-Lavigne, M. (2003). The morphogen sonic hedgehog is an axonal chemoattractant that collaborates with netrin-1 in midline axon guidance. *Cell* **113**, 11-23.

Charron, F. and Tessier-Lavigne, M. (2005). Novel brain wiring functions for classical morphogens: a role as graded positional cues in axon guidance. *Development* **132**, 2251-62.

Chen, M. H., Li, Y. J., Kawakami, T., Xu, S. M. and Chuang, P. T. (2004). Palmitoylation is required for the production of a soluble multimeric Hedgehog protein complex and long-range signaling in vertebrates. *Genes Dev* **18**, 641-59.

de Celis, J. F. (1998). Positioning and differentiation of veins in the Drosophila wing. *Int J Dev Biol* **42**, 335-43.

Desbordes, S. C. and Sanson, B. (2003). The glypican Dally-like is required for Hedgehog signalling in the embryonic epidermis of Drosophila. *Development* **130**, 6245-55.

Diez del Corral, R., Aroca, P., Gómez-Skarmeta, J., Cavodeassi, F. and Modolell, J. (1999). The Iroquois homeodomain proteins are required to specify body wall identity in Drosophila. *Genes Dev* **13**, 1754-61.

Echelard, Y., Epstein, D. J., St-Jacques, B., Shen, L., Mohler, J., McMahon, J. A. and McMahon, A. P. (1993). Sonic hedgehog, a member of a family of putative signaling molecules, is implicated in the regulation of CNS polarity. *Cell* **75**, 1417-30.

Entchev, E. V., Schwabedissen, A. and González-Gaitán, M. (2000). Gradient formation of the TGF-beta homolog Dpp. *Cell* **103**, 981-91.

Gallet, A., Rodriguez, R., Ruel, L. and Therond, P. P. (2003). Cholesterol modification of hedgehog is required for trafficking and movement, revealing an asymmetric cellular response to hedgehog. *Dev Cell* **4**, 191-204.

Gallet, A. and Therond, P. P. (2005). Temporal modulation of the Hedgehog morphogen gradient by a patched-dependent targeting to lysosomal compartment. *Dev Biol* **277**, 51-62.

García-Bellido, A., Ripoll, P. and Morata, G. (1973). Developmental compartmentalisation of the wing disk of Drosophila. *Nat New Biol* **245**, 251-3.

Gibson, M. C., Lehman, D. A. and Schubiger, G. (2002). Lumenal transmission of decapentaplegic in Drosophila imaginal discs. *Dev Cell* **3**, 451-60.

Glise, B., Miller, C. A., Crozatier, M., Halbisen, M. A., Wise, S., Olson, D. J., Vincent, A. and Blair, S. S. (2005). Shifted, the Drosophila ortholog of Wnt inhibitory factor-1, controls the distribution and movement of Hedgehog. *Dev Cell* **8**, 255-66.

Gorfinkiel, N., Sierra, J., Callejo, A., Ibanez, C. and Guerrero, I. (2005). The Drosophila ortholog of the human Wnt inhibitor factor Shifted controls the diffusion of lipid-modified Hedgehog. *Dev Cell* **8**, 241-53.

Grigliatti, T. A., Hall, L., Rosenbluth, R. and Suzuki, D. T. (1973). Temperature-sensitive mutations in Drosophila melanogaster. XIV. A selection of immobile adults. *Mol Gen Genet* **120**, 107-14.

Guillen, I., Mullor, J. L., Capdevila, J., Sanchez-Herrero, E., Morata, G. and Guerrero, I. (1995). The function of engrailed and the specification of Drosophila wing pattern. *Development* **121**, 3447-56.

Han, C., Belenkaya, T. Y., Wang, B. and Lin, X. (2004). Drosophila glypicans control the cell-to-cell movement of Hedgehog by a dynamin-independent process. *Development* **131**, 601-11.

Han, C., Yan, D., Belenkaya, T. Y. and Lin, X. (2005). Drosophila glypicans Dally and Dally-like shape the extracellular Wingless morphogen gradient in the wing disc. *Development* **132**, 667-79.

Harfe, B. D., Scherz, P. J., Nissim, S., Tian, H., McMahon, A. P. and Tabin, C. J. (2004). Evidence for an expansion-based temporal Shh gradient in specifying vertebrate digit identities. *Cell* **118**, 517-28.

Heemskerk, J. and DiNardo, S. (1994). Drosophila hedgehog acts as a morphogen in cellular patterning. *Cell* **76**, 449-60.

Incardona, J. P. and Eaton, S. (2000). Cholesterol in signal transduction. *Curr Opin Cell Biol* **12**, 193-203.

Ingham, P. W. and McMahon, A. P. (2001). Hedgehog signaling in animal development: paradigms and principles. *Genes Dev* **15**, 3059-87.

Kohtz, J. D., Lee, H. Y., Gaiano, N., Segal, J., Ng, E., Larson, T., Baker, D. P., Garber, E. A., Williams, K. P. and Fishell, G. (2001). N-terminal fatty-acylation of sonic hedgehog enhances the induction of rodent ventral forebrain neurons. *Development* **128**, 2351-63.

Koziel, L., Kunath, M., Kelly, O. G. and Vortkamp, A. (2004). Ext1-dependent heparan sulfate regulates the range of Ihh signaling during endochondral ossification. *Dev Cell* **6**, 801-13.

Lander, A. D., Nie, Q. and Wan, F. Y. (2002). Do morphogen gradients arise by diffusion? *Dev Cell* **2**, 785-96.

Lee, J. D., Kraus, P., Gaiano, N., Nery, S., Kohtz, J., Fishell, G., Loomis, C. A. and Treisman, J. E. (2001). An acylatable residue of Hedgehog is differentially required in Drosophila and mouse limb development. *Dev Biol* **233**, 122-36.

Lee, J. D. and Treisman, J. E. (2001). Sightless has homology to transmembrane acyltransferases and is required to generate active Hedgehog protein. *Curr Biol* **11**, 1147-52.

Lee, J. J., Ekker, S. C., von Kessler, D. P., Porter, J. A., Sun, B. I. and Beachy, P. A. (1994). Autoproteolysis in hedgehog protein biogenesis. *Science* **266**, 1528-37.

Lee, T. and Luo, L. (1999). Mosaic analysis with a repressible cell marker for studies of gene function in neuronal morphogenesis. *Neuron* **22**, 451-61.

Lewis, K. E. and Eisen, J. S. (2001). Hedgehog signaling is required for primary motoneuron induction in zebrafish. *Development* **128**, 3485-95.

Lewis, P. M., Dunn, M. P., McMahon, J. A., Logan, M., Martin, J. F., St-Jacques, B. and McMahon, A. P. (2001). Cholesterol modification of sonic hedgehog is required for long-range signaling activity and effective modulation of signaling by Ptc1. *Cell* **105**, 599-612.

Lin, X. (2004). Functions of heparan sulfate proteoglycans in cell signaling during development. *Development* **131**, 6009-21.

Lum, L., Yao, S., Mozer, B., Rovescalli, A., Von Kessler, D., Nirenberg, M. and Beachy, P. A. (2003). Identification of Hedgehog pathway components by RNAi in Drosophila cultured cells. *Science* **299**, 2039-45.

Ma, C., Zhou, Y., Beachy, P. A. and Moses, K. (1993). The segment polarity gene hedgehog is required for progression of the morphogenetic furrow in the developing Drosophila eye. *Cell* **75**, 927-38.

Mann, R. K. and Beachy, P. A. (2004). Novel lipid modifications of secreted protein signals. *Annu Rev Biochem* **73**, 891-923.

Marti, E., Bumcrot, D. A., Takada, R. and McMahon, A. P. (1995). Requirement of 19K form of Sonic hedgehog for induction of distinct ventral cell types in CNS explants [see comments]. *Nature* **375**, 322-5.

McMahon, A. P., Ingham, P. W. and Tabin, C. J. (2003). Developmental roles and clinical significance of hedgehog signaling. *Curr Top Dev Biol* **53**, 1-114.

Micchelli, C. A., The, I., Selva, E., Mogila, V. and Perrimon, N. (2002). Rasp, a putative transmembrane acyltransferase, is required for Hedgehog signaling. *Development* **129**, 843-51.

Motzny, C. K. and Holmgren, R. (1995). The Drosophila cubitus interruptus protein and its role in the wingless and hedgehog signal transduction pathways. *Mech Dev* **52**, 137-50.

Mullor, J. L. and Guerrero, I. (2000). A gain-of-function mutant of patched dissects different responses to the Hedgehog gradient. *Dev Biol* **228**, 211-224.

Munro, S. and Freeman, M. (2000). The notch signalling regulator fringe acts in the Golgi apparatus and requires the glycosyltransferase signature motif DXD. *Curr Biol* **10**, 813-20.

Ohlmeyer, J. T. and Kalderon, D. (1998). Hedgehog stimulates maturation of Cubitus interruptus into a labile transcriptional activator. *Nature* **396**, 749-53.

Pallavi, S. K. and Shashidhara, L. S. (2003). Egfr/Ras pathway mediates interactions between peripodial and disc proper cells in Drosophila wing discs. *Development* **130**, 4931-41.

Patel, N. H., Kornberg, T. B. and Goodman, C. S. (1989). Expression of engrailed during segmentation in grasshopper and crayfish. *Development* **107**, 201-12.

Pepinsky, R. B., Zeng, C., Wen, D., Rayhorn, P., Baker, D. P., Williams, K. P., Bixler, S. A., Ambrose, C. M., Garber, E. A., Miatkowski, K. et al. (1998). Identification of a palmitic acid-modified form of human Sonic hedgehog. *J Biol Chem* **273**, 14037-45.

Peters, C., Wolf, A., Wagner, M., Kuhlmann, J. and Waldmann, H. (2004). The cholesterol membrane anchor of the Hedgehog protein confers stable membrane association to lipid-modified proteins. *Proc Natl Acad Sci U S A* **101**, 8531-6.

Pignoni, F. and Zipursky, S. L. (1997). Induction of Drosophila eye development by decapentaplegic. *Development* **124**, 271-8.

Porter, J. A., Ekker, S. C., Park, W. J., von Kessler, D. P., Young, K. E., Chen, C. H., Ma, Y., Woods, A. S., Cotter, R. J., Koonin, E. V. et al. (1996a). Hedgehog patterning activity: role of a lipophilic modification mediated by the carboxy-terminal autoprocessing domain. *Cell* **86**, 21-34.

Porter, J. A., von, K. D., Ekker, S. C., Young, K. E., Lee, J. J., Moses, K. and Beachy, P. A. (1995). The product of hedgehog autoproteolytic cleavage active in local and long-range signalling. *Nature* **374**, 363-6.

Porter, J. A., Young, K. E. and Beachy, P. A. (1996b). Cholesterol modification of hedgehog signaling proteins in animal development. *Science* **274**, 255-9.

Rietveld, A., Neutz, S., Simons, K. and Eaton, S. (1999). Association of sterol- and glycosylphosphatidylinositol-linked proteins with Drosophila raft lipid microdomains. *J Biol Chem* **274**, 12049-54.

Sanchez-Herrero, E., Couso, J. P., Capdevila, J. and Guerrero, I. (1996). The fu gene discriminates between pathways to control dpp expression in Drosophila imaginal discs. *Mech Dev* **55**, 159-70.

Sevrioukov, E. A., He, J. P., Moghrabi, N., Sunio, A. and Kramer, H. (1999). A role for the deep orange and carnation eye color genes in lysosomal delivery in Drosophila. *Mol Cell* **4**, 479-86.

Shestopal, S. A., Makunin, I. V., Belyaeva, E. S., Ashburner, M. and Zhimulev, I. F. (1997). Molecular characterization of the deep orange (dor) gene of Drosophila melanogaster. *Mol Gen Genet* **253**, 642-8.

Strigini, M. and Cohen, S. M. (2000). Wingless gradient formation in the Drosophila wing. *Curr Biol* **10**, 293-300.

Tabata, T. and Kornberg, T. B. (1994). Hedgehog is a signaling protein with a key role in patterning Drosophila imaginal discs. *Cell* **76**, 89-102.

Tabata, T. and Takei, Y. (2004). Morphogens, their identification and regulation. *Development* **131**, 703-12.

Takei, Y., Ozawa, Y., Sato, M., Watanabe, A. and Tabata, T. (2004). Three Drosophila EXT genes shape morphogen gradients through synthesis of heparan sulfate proteoglycans. *Development* **131**, 73-82.

Tanimoto, H., Itoh, S., ten Dijke, P. and Tabata, T. (2000). Hedgehog creates a gradient of DPP activity in Drosophila wing imaginal discs. *Mol Cell* **5**, 59-71.

The, I., Bellaiche, Y. and Perrimon, N. (1999). Hedgehog movement is regulated through tout velu-dependent synthesis of a heparan sulfate proteoglycan. *Mol Cell* **4**, 633-9.

Therond, P. P., Limbourg Bouchon, B., Gallet, A., Dussilol, F., Pietri, T., van den Heuvel, M. and Tricoire, H. (1999). Differential requirements of the fused kinase for hedgehog signalling in the Drosophila embryo. *Development* **126**, 4039-51.

Tian, H., Jeong, J., Harfe, B. D., Tabin, C. J. and McMahon, A. P. (2005). Mouse Disp1 is required in sonic hedgehog-expressing cells for paracrine activity of the cholesterol-modified ligand. *Development* **132**, 133-42.

Torroja, C., Gorfinkiel, N. and Guerrero, I. (2004). Patched controls the Hedgehog gradient by endocytosis in a dynamin-dependent manner, but this internalization does not play a major role in signal transduction. *Development* **131**, 2395-408.

Torroja, C., Gorfinkiel, N. and Guerrero, I. (2005). Mechanisms of Hedgehog gradient formation and interpretation. *J Neurobiol* **64**, 334-56.

Vervoort, M., Crozatier, M., Valle, D. and Vincent, A. (1999). The COE transcription factor collier is a mediator of short-range hedgehog-induced patterning of the drosophila wing. *Curr Biol* **9**, 632-9.

Zecca, M., Basler, K. and Struhl, G. (1995). Sequential organizing activities of engrailed, hedgehog and decapentaplegic in the Drosophila wing. *Development* **121**, 2265-78.

Zeng, X., Goetz, J. A., Suber, L. M., Scott, W. J., Jr., Schreiner, C. M. and Robbins, D. J. (2001). A freely diffusible form of Sonic hedgehog mediates long-range signalling. *Nature* **411**, 716-20.

Zhu, A. J., Zheng, L., Suyama, K. and Scott, M. P. (2003). Altered localization of Drosophila Smoothened protein activates Hedgehog signal transduction. *Genes Dev* **17**, 1240-52.

Figure Legends

Figure 1. The large punctate structures of Hh, HhN and Hhc85s are endocytic vesicles and only the lipid-modified Hh forms oligomers in *Drosophila*

(A) Glycerol gradients (50-15%) used to fractionate Hh-GFP, HhN-GFP, Hhc85s-GFP and Hhc85sN-GFP obtained from salivary glands expressing the four Hh forms. We observed that wild type Hh fractionated as two different density gradients; one associated with the high molecular weight fraction (9-14), which corresponded to oligomers, and the other associated with the low molecular weight fraction (17-23), corresponding to monomers. HhN-GFP, Hhc85s-GFP, and Hhc85sN-GFP elute with the low-density fractions (monomers).

(B-D and b-d) Wing imaginal discs expressing the different Hh-GFP forms with the *hh-Gal4* driver. Hh-GFP forms a short gradient of around 6-7 cell diameters (blue line in B) while HhN-GFP and Hhc85s-GFP proteins are unable to generate a proper gradient (blue line in C and D). Note the presence of HhN-GFP and Hhc85s-GFP vesicles far from the Hh expressing cells.

Internalized dextran-red positive vesicles (24 minutes of incubation) co-localized with Hh-GFP (B), HhN-GFP (C) and Hhc85s-GFP (D) in both A and P compartments of the wing imaginal cells that expressed the three forms of Hh in their own expression domain using the Hh-Gal4 driver (arrowheads). Note that some GFP labeled particles do not co-localize with the internalized dextran (arrows). These particles are nevertheless intracellular (see Fig S1D). These results indicate that in all cases the punctate structures are endocytic vesicles. In all figures, the A/P boundary is indicated with a dotted line; the A compartment is always orientated to the left and the P compartment to the right.

Figure 2. Differential accumulation of Hh-GFP versus HhN-GFP and Hhc85s-GFP in the plasma membrane of *shi*^{ts1} mutant clones

(A-E) *shi*^{ts1}mutant clones induced in UAS-Hh /HhGal4 (A, D), UAS-HhN-GFP/HhGal4 (B,E), and Hhc85s-GFP/HhGal4 (C) wing imaginal discs. Hh-GFP accretions were only observed in the baso-lateral plasma membrane of the A compartment cells (arrowheads in A) while HhN-GFP (B) and Hhc85s-GFP (C) were only detected in the apical part of the A compartment cells. (D,E) Transverse sections of the *shi*^{ts1}mutant clones in A (D) and B (E). Arrows indicate the apical parts and arrowheads the baso-lateral parts of the cells. Note the baso-lateral accumulation of Hh (D) and the apical accumulation of HhN (E).

Figure 3. Differential localization of Hh-GFP, HhN-GFP and Hhc85s-GFP in the plasma membrane

(A-C) Extracellular labeling of Hh-GFP (A), Hhc85s-GFP (B), and HhN-GFP (C) showing their distribution at the apical versus baso-lateral plane. (a-c) A/P Z sections of the same wing discs in panels A, B and C. (a') A/P Z sections of a wing disc double-stained with anti- Hh antibody (green) and anti- DE-cadherin (blue) as an apical region marker. The three Hh forms occur in the extracellular space on the apical side of the producing cells (asterisk), while only lipid-unmodified forms of Hh appear in the apical extracellular space in the A compartment (arrows in apical planes and Z sections). Wild type Hh forms an extracellular gradient in the baso-lateral A cells next to the A/P compartment, while the lipid-unmodified forms are poorly represented and do not form a gradient (arrowheads in baso-lateral panels and Z sections).

Figure 4. Internalization and degradation of HhN and Hhc85s independent of Ptc

(A-C) *dor*^{8} clones induced in UAS-Hh /HhGal4 (A), HhN-GFP/HhGal4 (B), and Hhc85s-

GFP/HhGal4 (C) wing discs. The graphs represent a normalized pixel intensity of Ptc, Hh and β-Gal staining, measured in the area represented by white frames in panels A, B and C. The three forms of Hh accumulate in *dor*^{8} clones, indicating an active process of degradation. Note the precise direct correlation between the amounts of accumulated wild type Hh and Ptc in panel A (see graph) and, compared to that of the lipid-unmodified Hh forms, the absence of Ptc accumulation in panels B and C (see graph).

(D-F) *dor*$^{8-}$ clones in *ap-Gal4* / UAS-Hh-GFP (D), *ap-Gal4* / UAS-HhN-GFP (E) and *ap-Gal4* / UAS-Hhc85s-GFP (F) wing imaginal discs. There is increased accumulation of HhN-GFP and Hhc85s-GFP in *dor*$^{-}$ clones, induced both in the A and P compartments, even when they are located far from their expressing domains (arrows in E and F). However, wild type Hh-GFP accumulates in a very short range in A compartment *dor*$^{-}$ clones (arrows in D) and is never accumulated in P compartment *dor*$^{-}$ clones (arrowheads in D). The accumulation of HhN-GFP and Hhc85s-GFP (green) in the P compartment *dor*$^{-}$ cells, where Ptc (red) is not present, indicates a process of internalization and degradation independent of Ptc (arrowheads in E and D). This is reinforced by the absence of Ptc accumulation in A compartment *dor*$^{-}$ clones in the case of Hhc85s-GFP (arrows in F). In the case of HhN-GFP, the small amount of Ptc accumulation in *dor*$^{-}$ clones induced in the A compartment reveals some interaction between HhN and the Ptc receptor (arrows in E). The graphs on the right-hand side of the figure represent the areas of the disc shown in the confocal panels and the interpretation of the results shown.

Figure 5. Inductive effect of HhN but not of Hh from peripodial cells upon disc proper cells

(A-C') Expression of Hh-GFP (A,a and A',a'), HhN-GFP (B,b and B',b'), and Hhc85s-GFP (C,c and C',c') in peripodial cells using the *Ubx-Gal4* driver. The Ubx is expressed at high

levels in the part of the peripodial membrane corresponding to the P compartment. Note that HhN-GFP and Hhc85s-GFP but not wild type Hh-GFP are observed in internalized vesicles in the disc proper cells (arrows) and that the internalized vesicles of HhN-GFP are more clearly visualized in the A than in the P compartment, unlike Hhc85s-GFP vesicles, which are visible in both A and P compartments. Dpp (red) is ectopically induced in the disc proper cells in HhN-GFP / *Ubx-Gal4* disc (B and B').

(D-G) Wing and notum phenotypes of the Hh-GFP/*Ubx-Gal4* and Hhc85s-GFP/*Ubx-Gal4* (D and F), HhN-GFP / *Ubx-Gal4* flies (E and G). Note the enlargement and extra-macroquetes of the notum and modification of the wing pattern in HhN-GFP / *Ubx-Gal4* flies.

(H) Diagrams showing the organization of the disc proper cells and peripodial cells in a front- and transverse view of a wing imaginal disc.

Figure 6. Signaling activity of Hh, HhN and Hhc85s

(A) Diagram of a wing imaginal disc with the posterior P compartment cells expressing Hh (green) and the anterior A compartment cell expressing Ptc (red) in response to Hh. The red frame indicates the territory represented in the adjacent panel, showing the real staining of the wing disc with Hh (green) and Ptc (red) antibodies. The right panel shows the expression of different Hh target genes in A compartment cells. The different thresholds of Hh signaling required for the activation of the different targets are indicated in the graph in (B).

Ectopic Hh-GFP (C-F), HhN-GFP (G-J) and Hhc85s-GFP (K-N) clones induce activation of En (C,G,K), Ptc (D,H,L), Dpp (E,I,M) and Iro (F,J,N) in the anterior compartment (labeled in red). Hh expressing cells are marked by ß-Gal (blue) in most of the panels, with the exception of panels E, I and M, where they are labeled by the absence of CD2. Arrows indicate the autonomous response and arrowheads the non-autonomous response to various forms of Hh.

(O,P,Q) Graphs represent the activation of Hh targets by ectopic Hh-GFP (O), HhN-GFP (P)

and Hhc85s-GFP (Q) clones in the A compartment. Light green coloring represents the levels and graded distribution of Hh protein and the dark green color represents the signaling activity of wild type Hh, HhN-GFP and Hhc85s-GFP. Note that in panel O, but not in panels P and Q, Hh protein distribution is the same as its signaling activity gradient.

Figure 7. Diffusion properties and signaling activity of Hh-GFP, HhN-GFP and Hhc85s-GFP in *ttv*$^{-}$ mutant cells

(A-K) *ttv*$^{-}$ clones labeled by the absence of β-Gal staining (blue) in wing discs expressing Hh-GFP (A, B, C), HhN-GFP (E, F, G) and Hhc85s-GFP (I, J, K) with the *hh-Gal4* driver (green) and stained for Ptc (A, E, I), Col (B, F, J) and Iro (C, G, K) in red. Note that HhN-GFP and Hhc85s-GFP but not wild type Hh-GFP appear inside the *ttv*$^{-}$ cells and in the cells located anterior to the clone (arrows in E and I). Also note that Ptc and Col are expressed only in the first row of *ttv*$^{-}$ cells next to the A/P border (arrowheads in A, B, E, F, I and J) and Hh-GFP vesicles co-localize with Ptc in all cases (arrowheads in A, E, and I). Iro is expressed only in the first row of cells in the wild type Hh-GFP and Hhc85s-GFP expressing discs (arrows in C and K), while in HhN-GFP expressing discs, Iro is activated throughout the *ttv*$^{-}$ clone (arrowheads in G and clone 1 in H). However, Iro expression decreases in a clone far from the HhN-GFP producing cells because HhN-GFP levels are lower than at the A/P compartment border (arrow in G and clone 2 in H).

(D, H, L) Graphs showing the activation of Ptc, Col, and Iro in *ttv*$^{-}$ clones abutting the A/P compartment border (Clone 1) or located distant to the A/P border (clone 2) by wild type Hh-GFP (D), HhN-GFP (H) and Hhc85s-GFP (L). The light green represents Hh levels and the graded distribution of the protein produced in the P compartment and secreted to the A compartment; the dark green represents the signaling activity induced by the different Hh

forms. The dotted lines represent the Hh gradients and signaling activity in a disc that does not contain *ttv*$^{-}$ clones.

Figure 8. Signaling activity of Hh-GFP, HhN-GFP and Hhc85s-GFP in cells lacking *tout-velu* function and simultaneously expressing Hh

(A-D) Wing imaginal discs with clones mutant for *ttv* that also express wild type Hh ectopically. All clones in the anterior compartment shown in the figure are located outside the expression domain of the different target genes tested. Clones are marked with GFP (A-D) and outlined with red-colored line (A'-D'), and the discs are stained for different Hh targets (red): En (A, A'), Ptc (B, B'), Iro (C, C'), and Ci (D, D'). (E) Diagram summarizing the results of the clone analysis. Hh triggers the response of low-threshold responses (Ci and Iro) in *ttv*$^{-}$ cells, while failing to activate high-threshold response genes (Ptc, En and Col) apart from the first row of cells within the clone.

Figure S1. **Hh-GFP, HhN-GFP, Hhc85s-GFP and Hhc85sN-GFP are correctly processed and recognized by anti-Hh antibodies**

(A) Upper panel: Western blot using anti-Hh antibody of Hedgehog-GFP fusion protein and its mutant forms expressed in the salivary glands. This blot indicates that the Hh forms are correctly processed and are expressed at equivalent levels. Lower panel: Coomasie staining of the SDS-PAGE gel as a control of the amount of protein extract loaded for each sample.

(B, C) Ectopic HhN-GFP (B, b) and Hhc85s-GFP (C, c) clones showing the co-localization of protein-GFP and anti-Hh antibody (Takei et al., 2004). Note their co-localization in the punctate structures in both the A and P compartments. White frames in B and C indicate the territory represented in b and c respectively.

(D) Hh-GFP / *hh-Gal4* wing disc incubated with dextran-red to label the endocytic compartment and subsequently incubated with anti-GFP antibody at 4ºC to label the extracellular Hh-GFP (see Materials and Methods). Note that some Hh punctate structure (green), but not all, co-localize with dextrans (arrowheads) indicating that they are internalized vesicles. The punctate structures that do not co-localize with dextrans are also intracellular vesicles (arrows), because they are not labeled by extracellular staining.

Figure S2. Long-range diffusion and signaling of a single HhN-GFP ectopic clone induced in the disc proper cells.

(A, B) A wing imaginal disc containing a single HhN-GFP (green) ectopic clone. (A) This clone was induced in the disc proper cells and shows a long-range activation of Iro (red). (B) Peripodial cells of the same disc, marked by Ubx expression (blue), do not contain ectopic clones.

(C,D) A comparison of the diffusion range of HhN-GFP (the same ectopic clone shown in A,B) with that of Hh-GFP ectopic clone. Both ectopic clones, HhN-GFP (C) and Hh-GFP (D) are of equivalent size, position and expression levels. Note that the gradient produced by HhN-GFP is much extended than the one produced by Hh-GFP.

These data together with the ones shown in Figures 5 and 6 indicate that Hh-N forms a very extended gradient.

Figure S3. *ptc*$^{-}$, *ttv*$^{-}$, double mutant clones do not internalized Hh

(A) Apical view of confocal images of a *ttv*$^{-}$ clone (labeled by the absence of ß-gal in red) abutting the A/P border in a *UAS-Hh-GFP / hh-Gal4* wing imaginal disc showing the internalization of Hh-GFP in the first row of cells inside the clone touching the A/P border.

(B) *ptc*$^{-}$, *ttv*$^{-}$ double clones abutting the A/P border in a *UAS-Hh-GFP / hh-Gal4* wing

imaginal disc. Note the absence of Hh-GFP vesicles inside the *ptc*$^{-}$, *ttv*$^{-}$ clone.

Figure 1

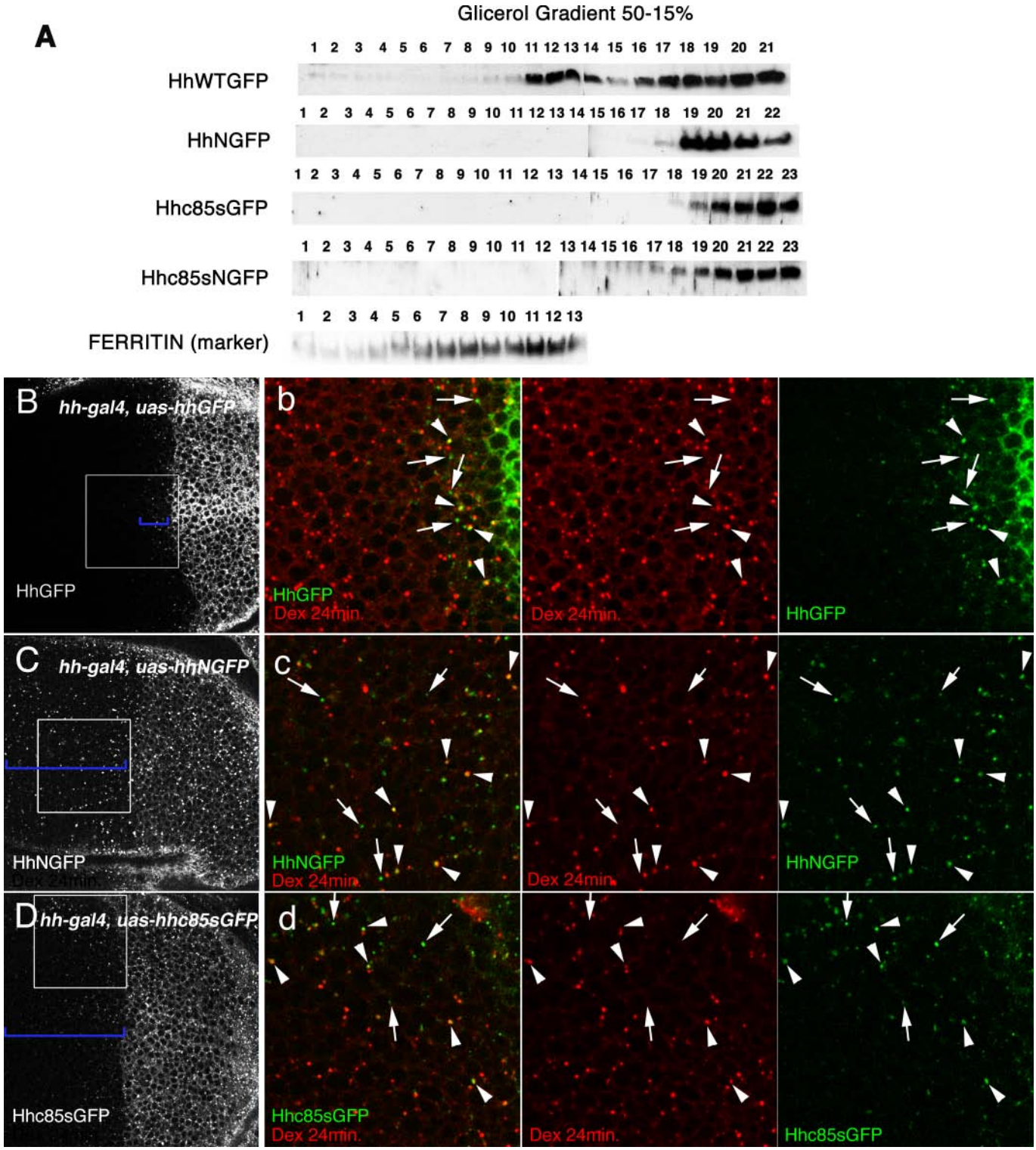
A
Glicerol Gradient 50-15%
HhWTGFP
HhNGFP
Hhc85sGFP
Hhc85sNGFP
FERRITIN (marker)
B hh-gal4, uas-hhGFP
HhGFP
b
HhGFP
Dex 24min.
Dex 24min.
HhGFP
C hh-gal4, uas-hhNGFP
HhNGFP
c
HhNGFP
Dex 24min.
Dex 24min.
HhNGFP
D hh-gal4, uas-hhc85sGFP
Hhc85sGFP
d
Hhc85sGFP
Dex 24min.
Dex 24min.
Hhc85sGFP

Figure 2

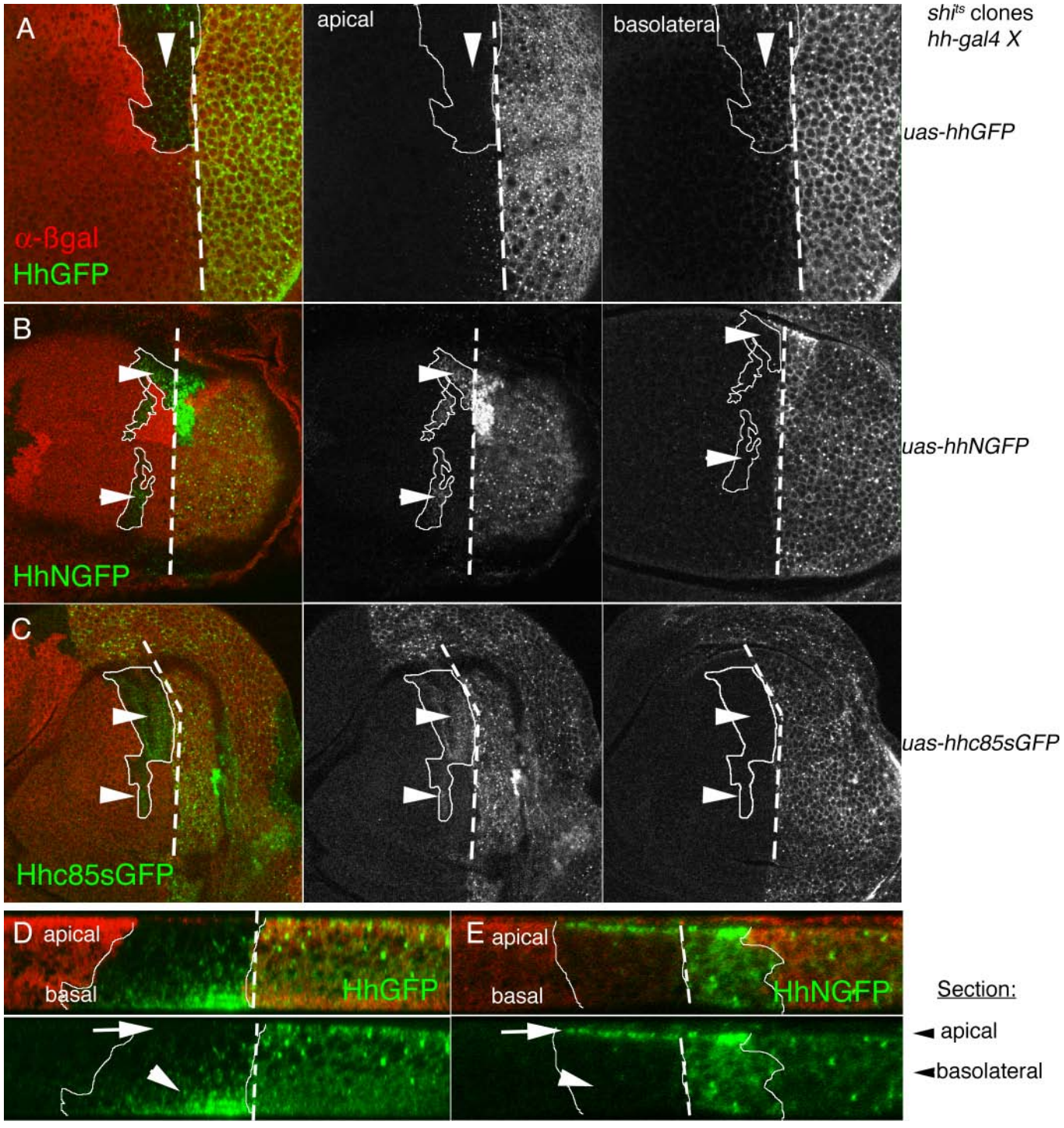
A
apical
basolatera
shi^ts clones
hh-gal4 X
uas-hhGFP
α-βgal
HhGFP
B
uas-hhNGFP
HhNGFP
C
uas-hhc85sGFP
Hhc85sGFP
D apical
basal
HhGFP
E apical
basal
HhNGFP
Section:
apical
basolateral

Figure 3

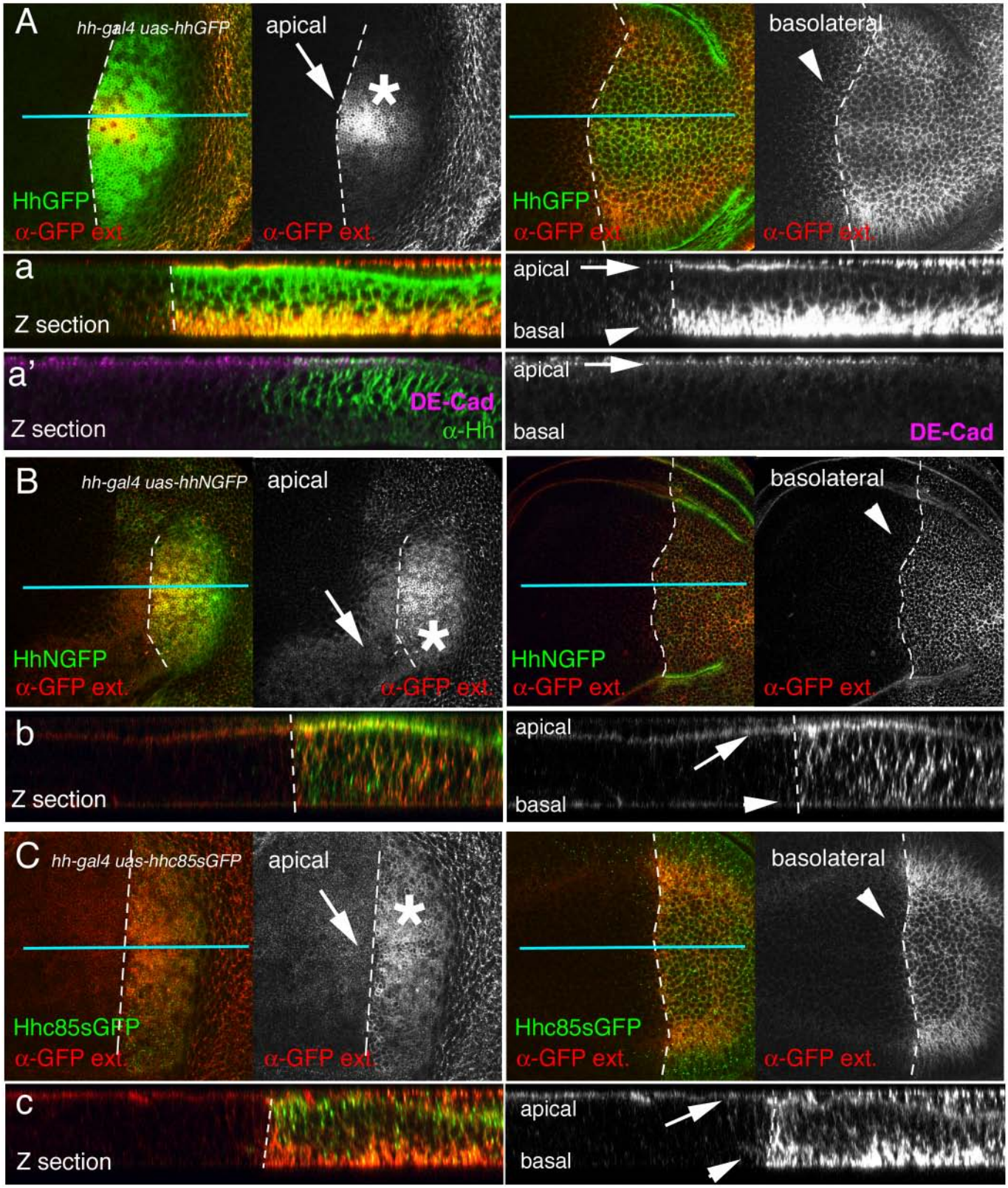
A
hh-gal4 uas-hhGFP
apical
basolateral
HhGFP
α-GFP ext.
a
Z section
apical
basal
a'
DE-Cad
α-Hh
B
hh-gal4 uas-hhNGFP
HhNGFP
b
C
hh-gal4 uas-hhc85sGFP
Hhc85sGFP
c

Figure 4

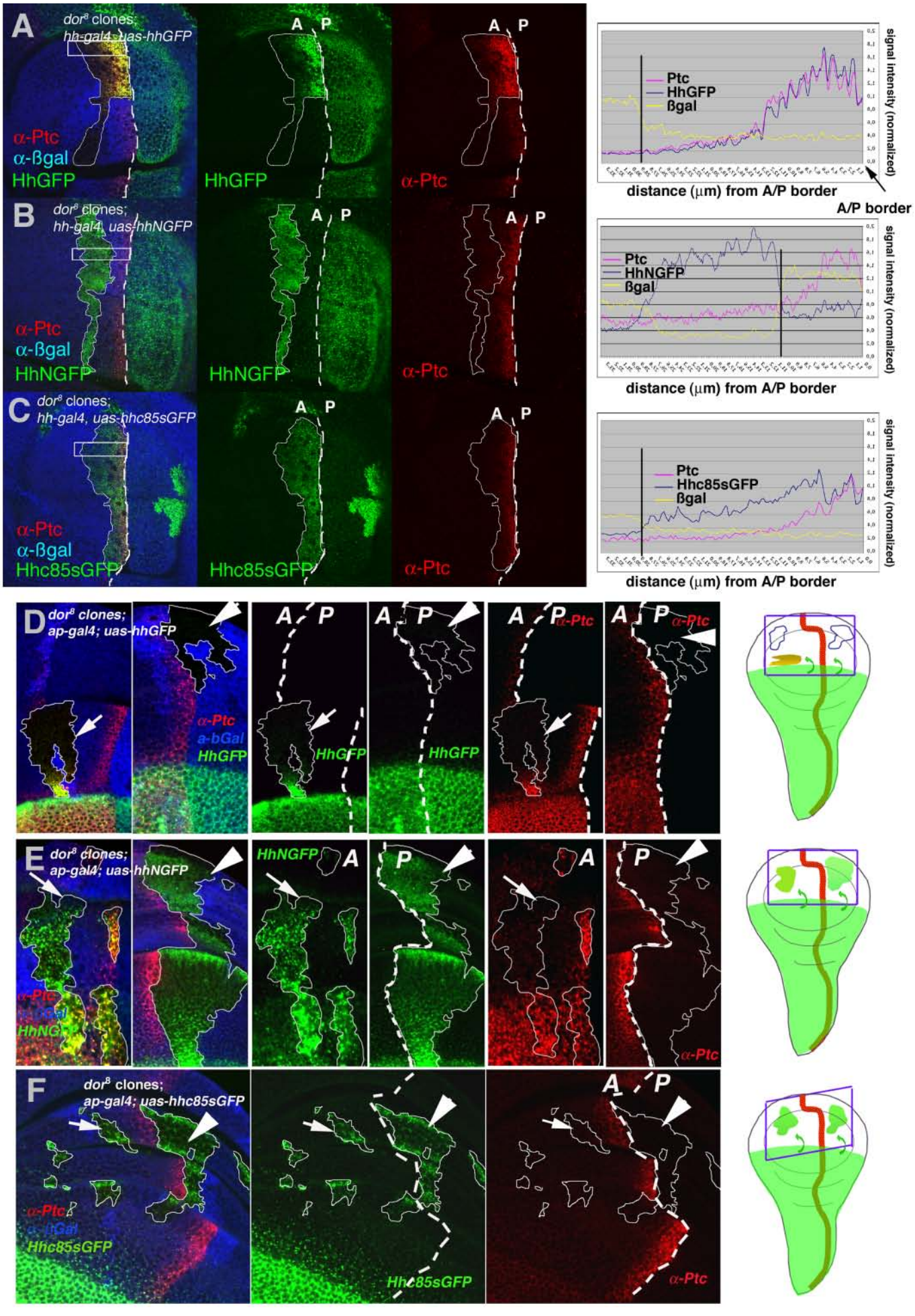
A
dor8 clones;
hh-gal4, uas-hhGFP
α-Ptc
α-ßgal
HhGFP
A P
HhGFP
α-Ptc
Ptc
HhGFP
ßgal
signal intensity (normalized)
distance (μm) from A/P border
A/P border
B
dor8 clones;
hh-gal4, uas-hhNGFP
α-Ptc
α-ßgal
HhNGFP
HhNGFP
α-Ptc
Ptc
HhNGFP
ßgal
signal intensity (normalized)
distance (μm) from A/P border
C
dor8 clones;
hh-gal4, uas-hhc85sGFP
α-Ptc
α-ßgal
Hhc85sGFP
Hhc85sGFP
α-Ptc
Ptc
Hhc85sGFP
ßgal
signal intensity (normalized)
distance (μm) from A/P border
D
dor8 clones;
ap-gal4; uas-hhGFP
α-Ptc
a-bGal
HhGFP
HhGFP
α-Ptc
E
dor8 clones;
ap-gal4; uas-hhNGFP
HhNGFP
α-Ptc
F
dor8 clones;
ap-gal4; uas-hhc85sGFP
α-Ptc
Hhc85sGFP
Hhc85sGFP
α-Ptc

Figure 5

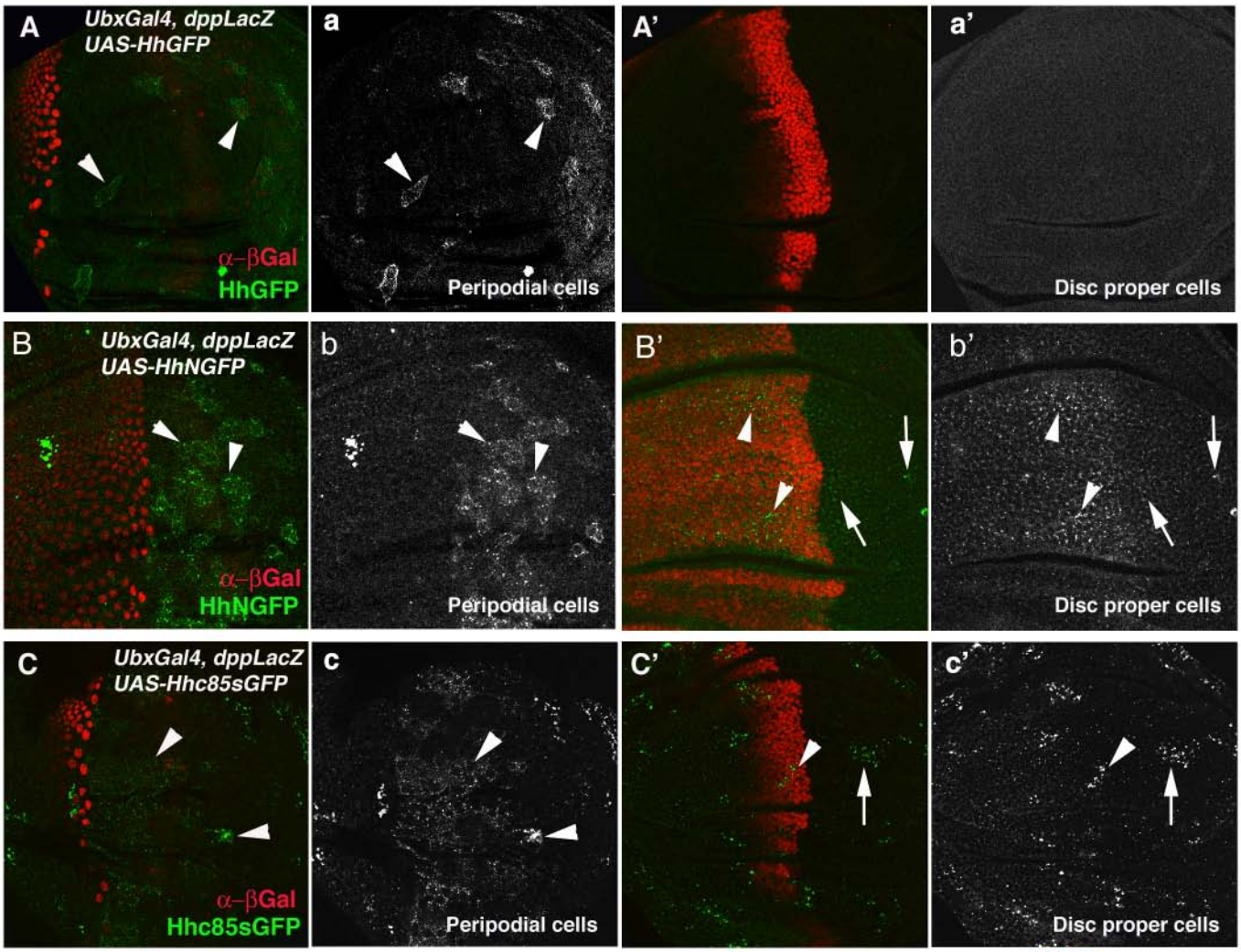
A
UbxGal4, dppLacZ
UAS-HhGFP
α–βGal
HhGFP
a
Peripodial cells
A'
a'
Disc proper cells
B
UbxGal4, dppLacZ
UAS-HhNGFP
α–βGal
HhNGFP
b
Peripodial cells
B'
b'
Disc proper cells
C
UbxGal4, dppLacZ
UAS-Hhc85sGFP
α–βGal
Hhc85sGFP
c
Peripodial cells
C'
c'
Disc proper cells


D
UbxGal4, dppLacZ X UAS-Hhc85sGFP

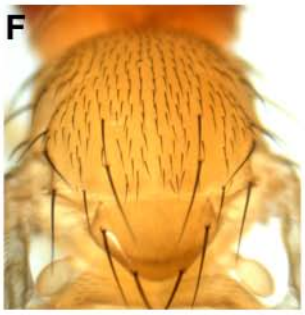
F

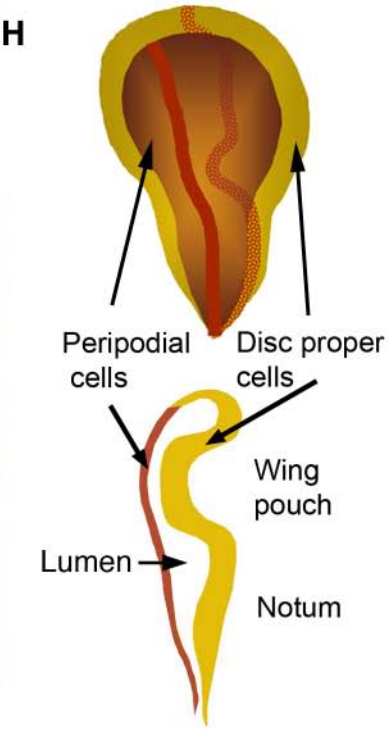
H
Peripodial cells
Disc proper cells
Wing pouch
Lumen
Notum

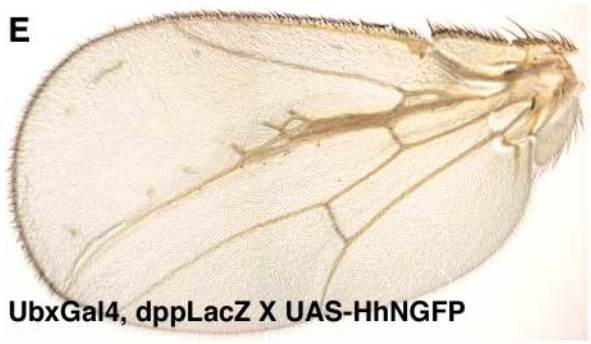
E
UbxGal4, dppLacZ X UAS-HhNGFP

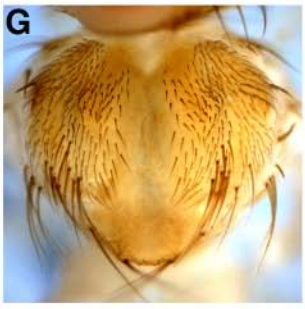
G

Figure 6

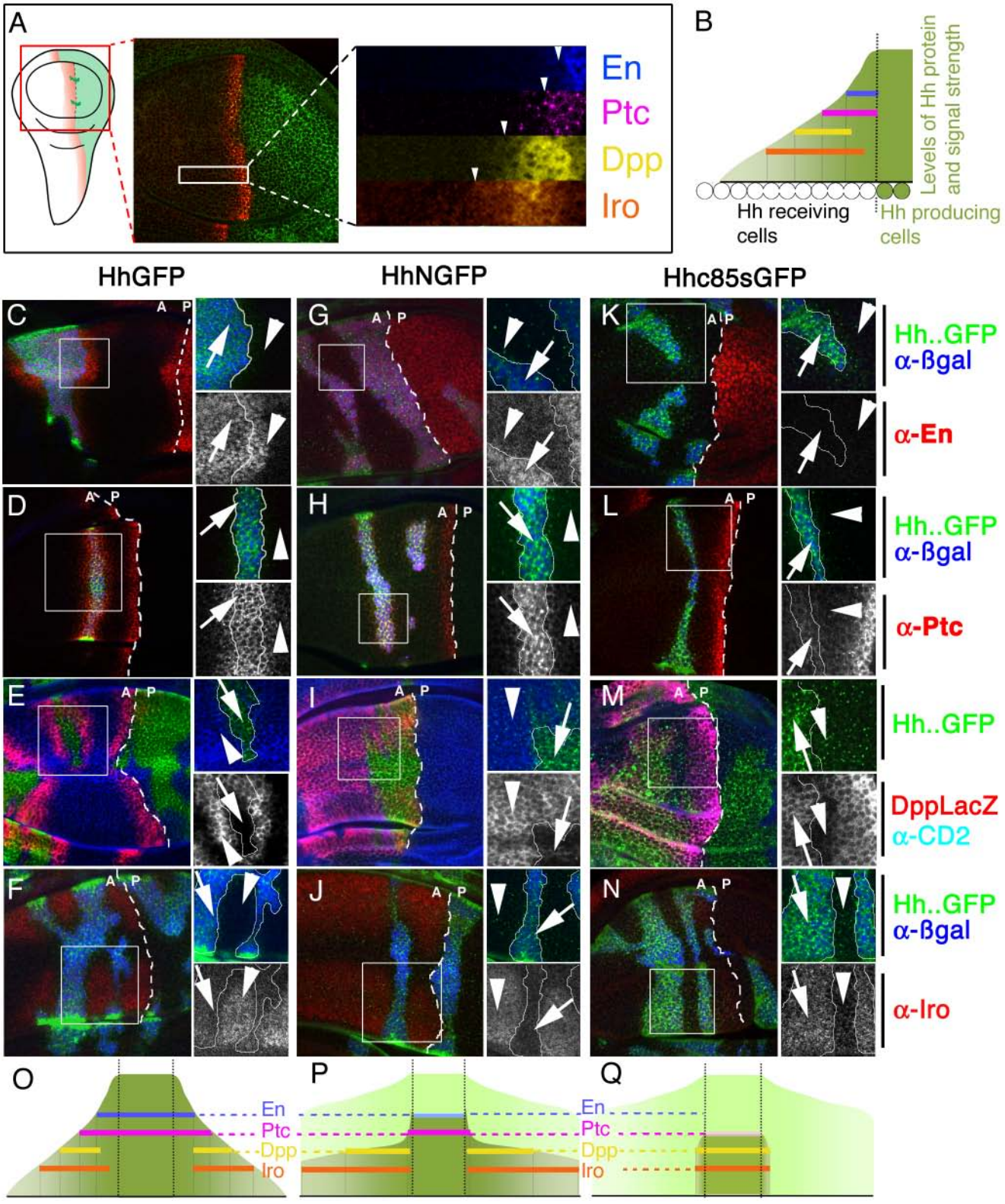
A
En
Ptc
Dpp
Iro
B
Levels of Hh protein and signal strength
Hh receiving cells
Hh producing cells
HhGFP
HhNGFP
Hhc85sGFP
C
D
E
F
G
H
I
J
K
L
M
N
A
P
Hh..GFP
α-βgal
α-En
α-Ptc
DppLacZ
α-CD2
α-Iro
O
P
Q
En
Ptc
Dpp
Iro

Figure 7

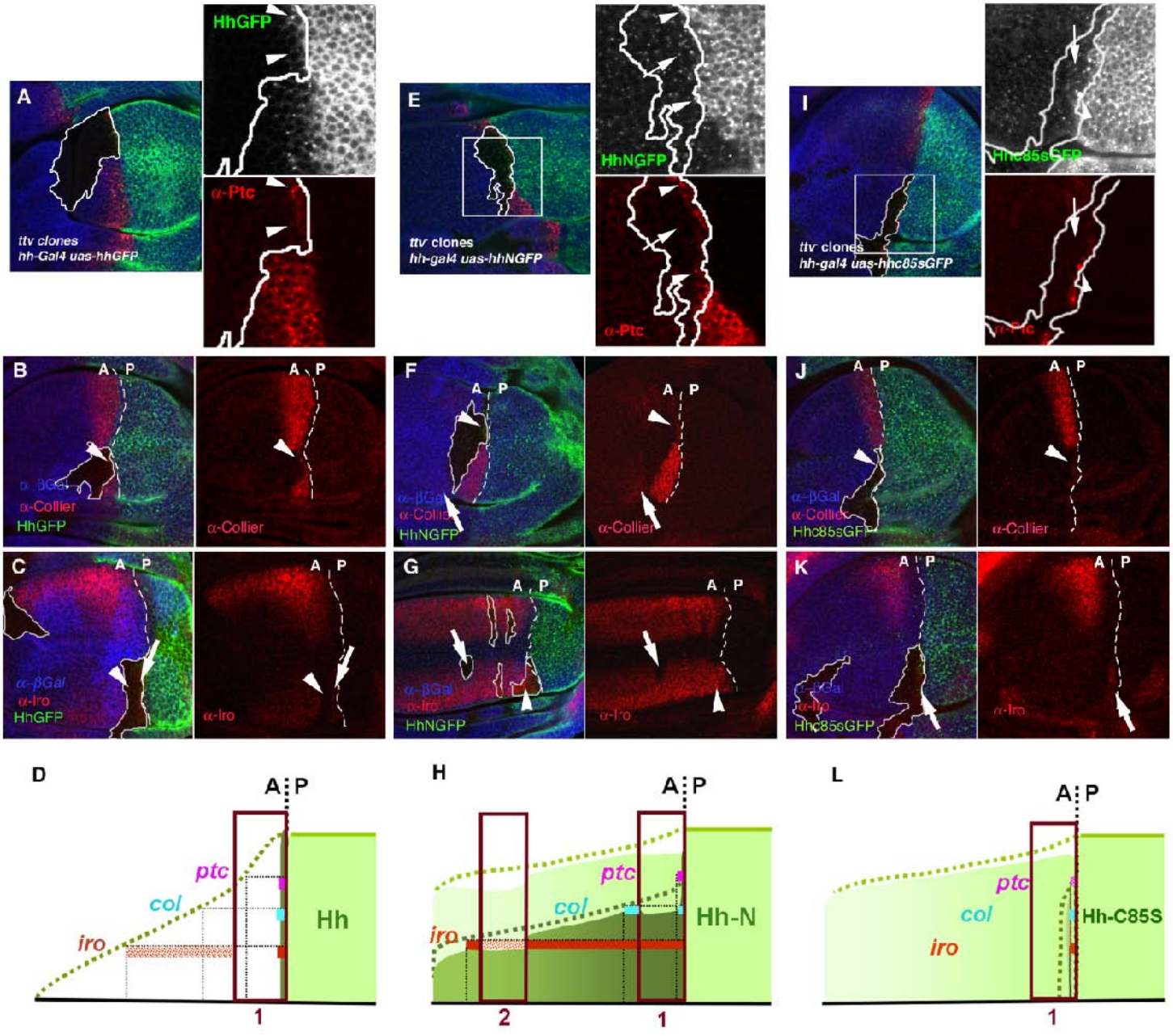
A
HhGFP
α-Ptc
ttv clones
hh-Gal4 uas-hhGFP
E
HhNGFP
α-Ptc
ttv clones
hh-gal4 uas-hhNGFP
I
Hhc85sGFP
ttv clones
hh-gal4 uas-hhc85sGFP
B
α-βGal
α-Collier
HhGFP
α-Collier
F
α-βGal
α-Collier
HhNGFP
α-Collier
J
α-βGal
α-Collier
Hhc85sGFP
α-Collier
C
α-βGal
α-Iro
HhGFP
α-Iro
G
α-βGal
α-Iro
HhNGFP
α-Iro
K
α-βGal
α-Iro
Hhc85sGFP
α-Iro
A
P
D
ptc
col
iro
Hh
1
H
ptc
col
iro
Hh-N
2
1
L
ptc
col
iro
Hh-C85S
1

Figure 8

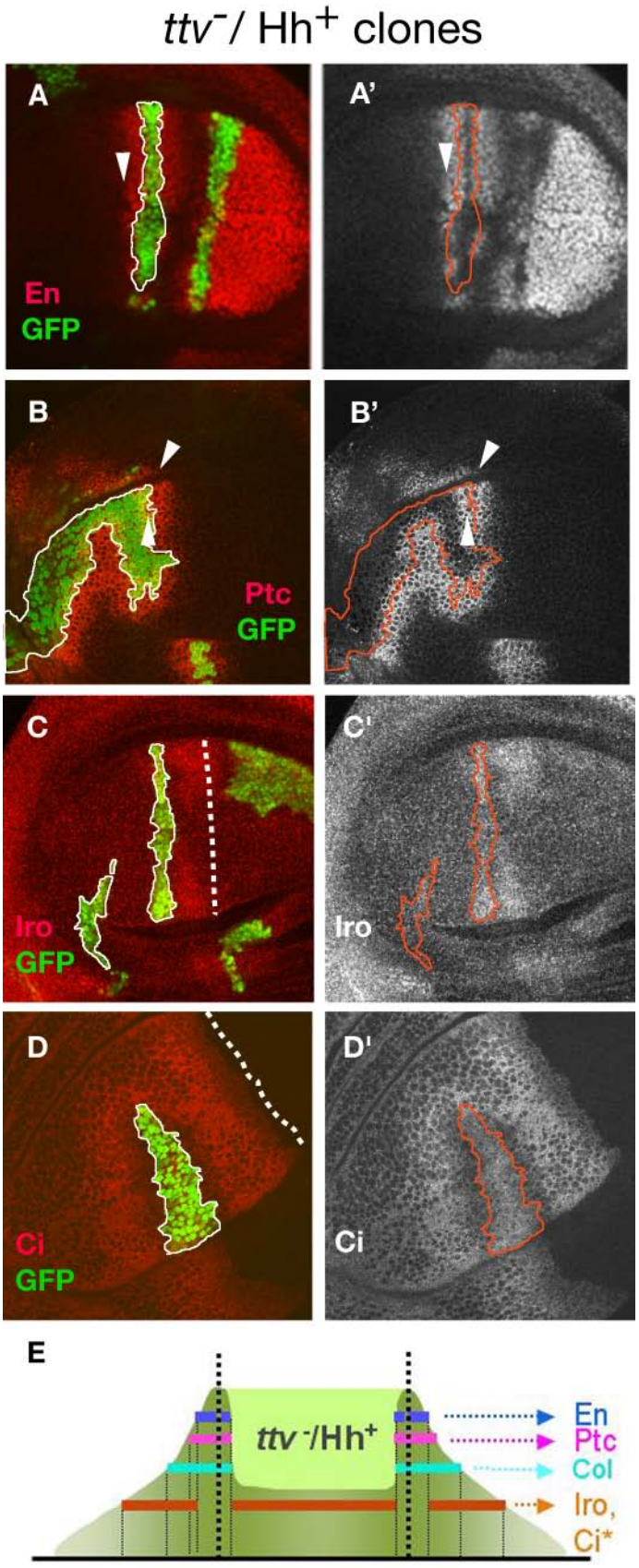
ttv⁻/ Hh⁺ clones
A
A'
En
GFP
B
B'
Ptc
GFP
C
C'
Iro
GFP
Iro
D
D'
Ci
GFP
Ci
E
ttv -/Hh+
En
Ptc
Col
Iro,
Ci*

Figure S1

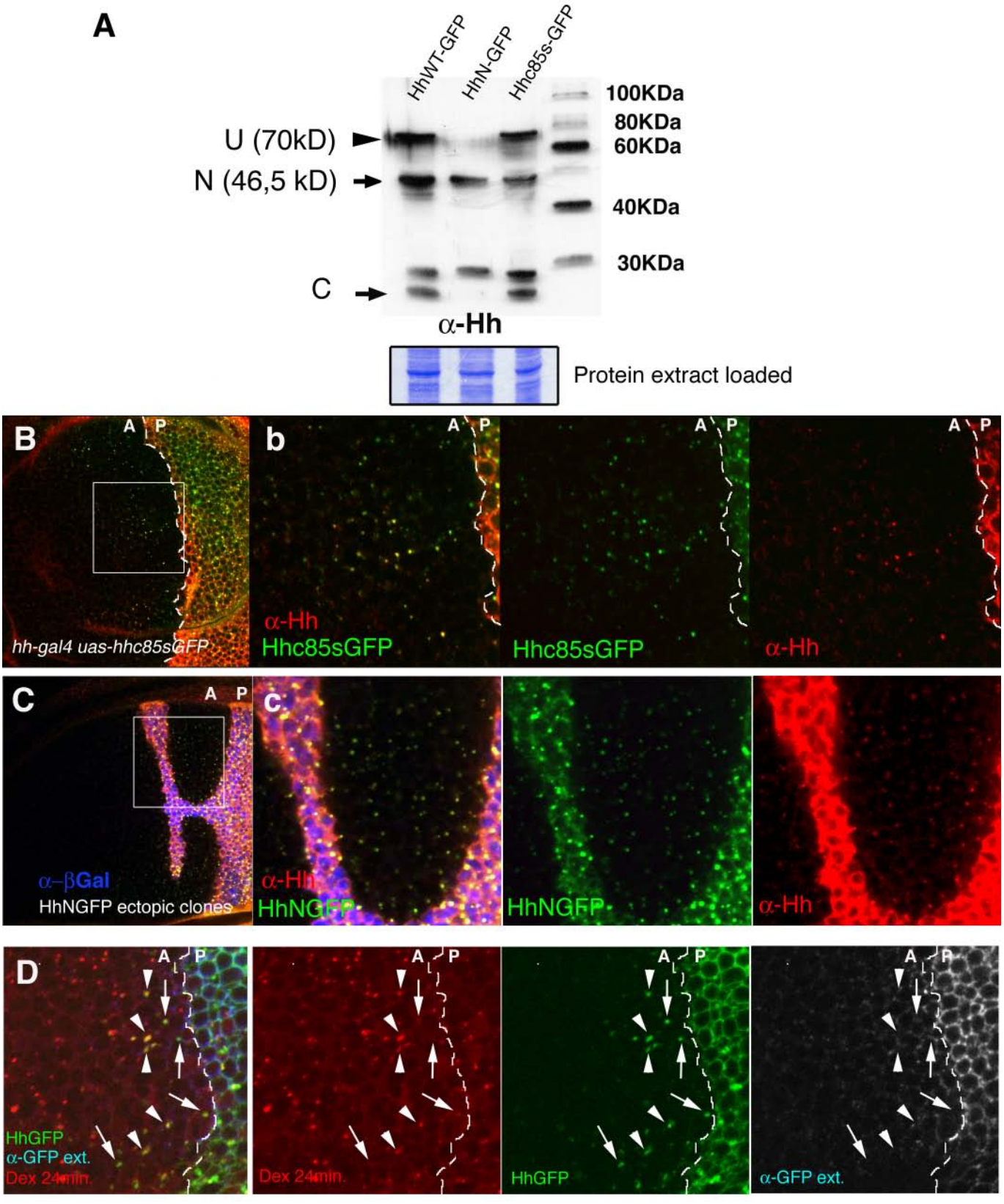
A
HhWT-GFP
HhN-GFP
Hhc85s-GFP
100KDa
80KDa
60KDa
40KDa
30KDa
U (70kD)
N (46,5 kD)
C
α-Hh
Protein extract loaded
B
A P
hh-gal4 uas-hhc85sGFP
b
α-Hh
Hhc85sGFP
Hhc85sGFP
α-Hh
C
α-βGal
HhNGFP ectopic clones
c
α-Hh
HhNGFP
HhNGFP
α-Hh
D
HhGFP
α-GFP ext.
Dex 24min.
Dex 24min.
HhGFP
α-GFP ext.

Figure S2

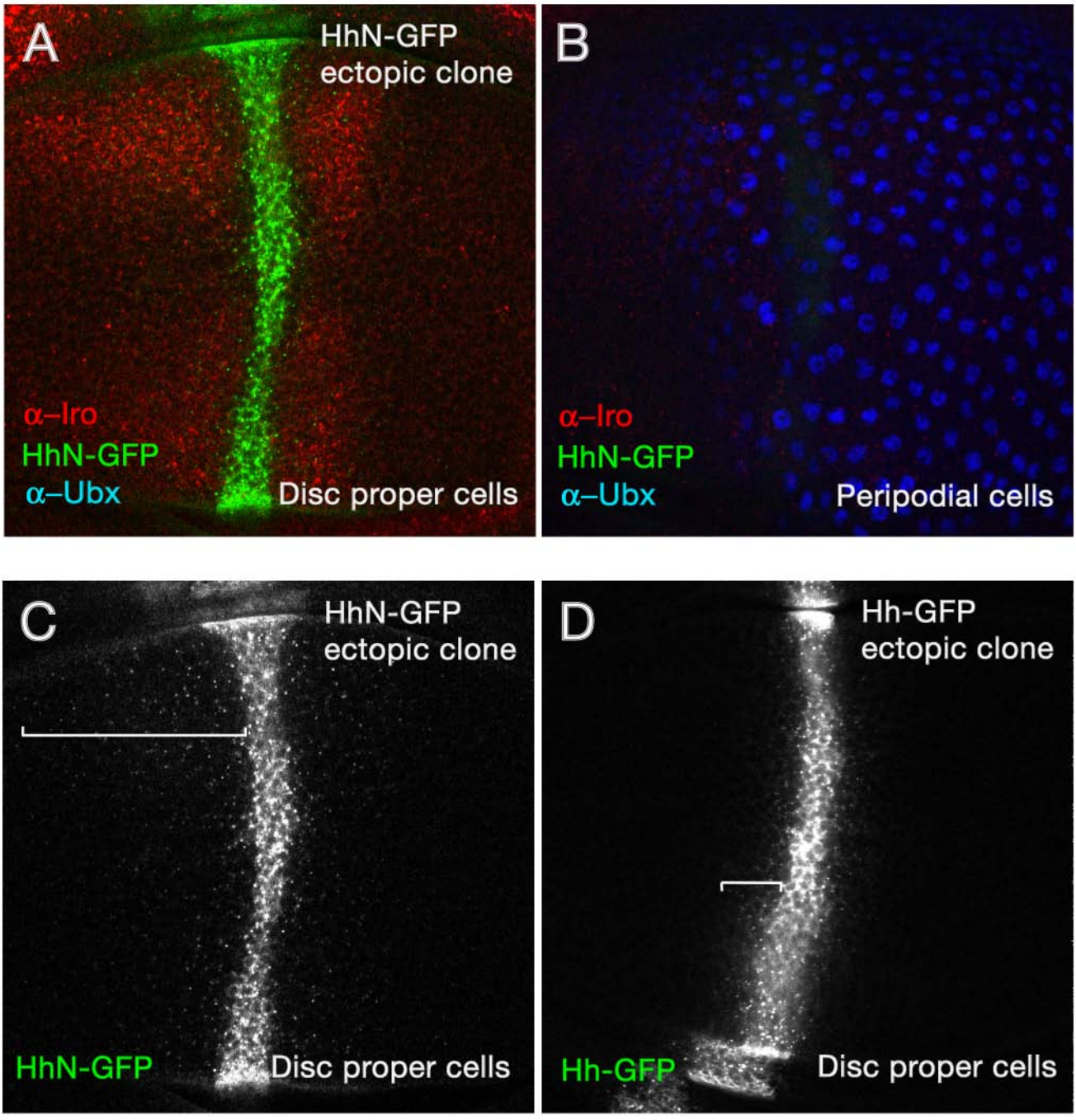
A
HhN-GFP
ectopic clone
α–Iro
HhN-GFP
α–Ubx
Disc proper cells
B
α–Iro
HhN-GFP
α–Ubx
Peripodial cells
C
HhN-GFP
ectopic clone
HhN-GFP
Disc proper cells
D
Hh-GFP
ectopic clone
Hh-GFP
Disc proper cells

Figure S3

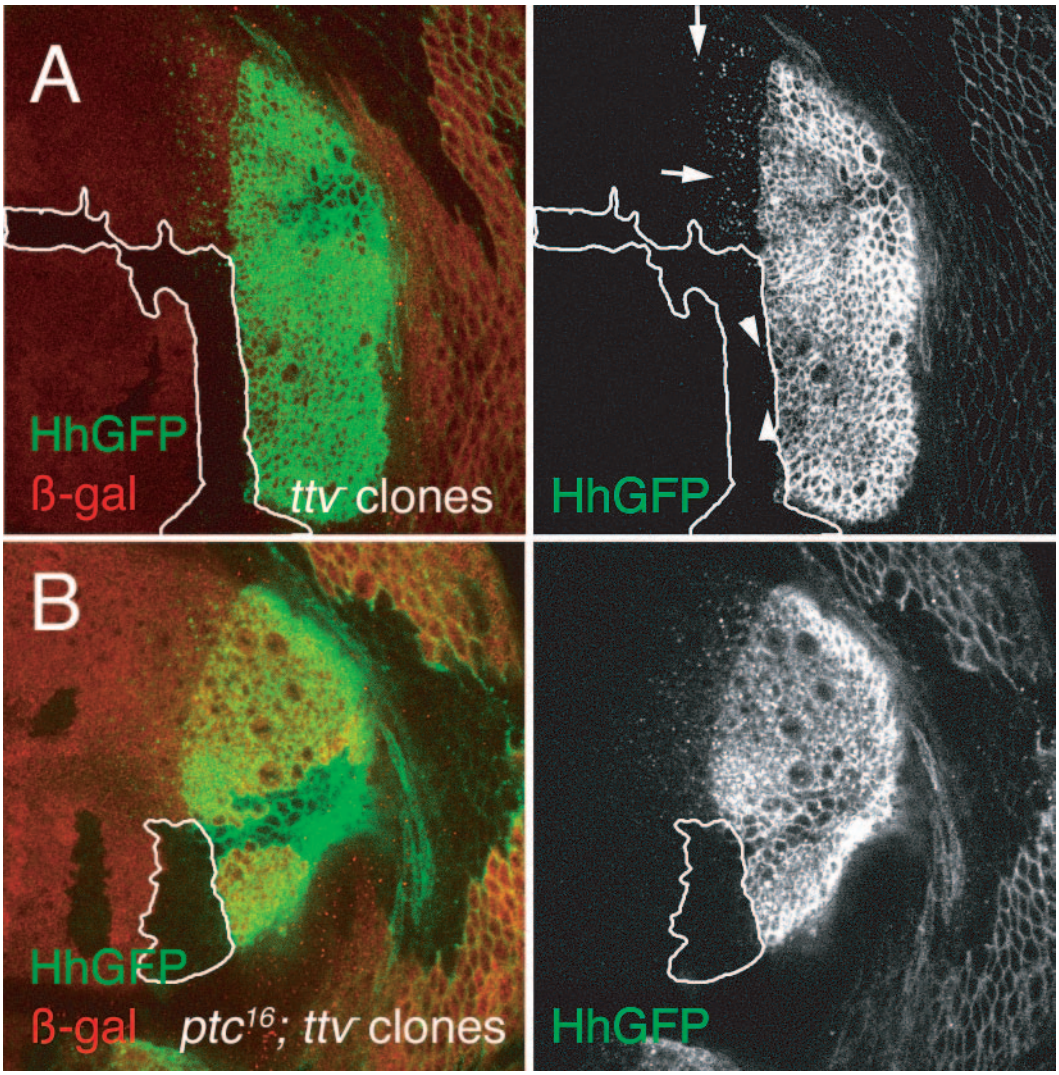
A
HhGFP
ß-gal
ttv clones
HhGFP
B
HhGFP
ß-gal
ptc16; ttv clones
HhGFP